Insight into the Composition of Organic Compounds ($\geq C_6$) in $PM_{2.5}$ in Wintertime in Beijing, China

Ruihe Lyu[1,2], Zongbo Shi[2], Mohammed Salim Alam[2], Xuefang Wu[2, 4], Di Liu[2], Tuan V. Vu[2], Christopher Stark[2], Pingqing Fu[3], Yinchang Feng[1] and Roy M. Harrison[2]†*

[1] State Environmental Protection Key Laboratory of Urban Ambient Air Particulate Matter Pollution Prevention and Control, College of Environmental Science and Engineering Nankai University, Tianjin 300350, China

[2] Division of Environmental Health and Risk Management School of Geography, Earth and Environmental Sciences, University of Birmingham Edgbaston, Birmingham B15 2TT, UK

[3] Institute of Surface Earth System Science, Tianjin University Tianjin, 300350, China

[4] Regional Department of Geology and Mineral Resources, China University of Geosciences, Xueyuan Road 29, 100083 Beijing China

† Also at: Department of Environmental Sciences / Centre of Excellence in Environmental Studies, King Abdulaziz University, PO Box 80203, Jeddah, 21589, Saudi Arabia

Corresponding author: E-mail: r.m.harrison@bham.ac.uk (Roy M. Harrison)

ABSTRACT

Organic matter is a major component of $PM_{2.5}$ in megacities. In order to understand the detailed characteristics of organic compounds ($\geq C_6$) at a molecular level on non-haze and haze days, we determined more than 300 organic compounds in the $PM_{2.5}$ from an urban area of Beijing collected in November-December 2016 using two-dimensional gas chromatography coupled to time-of-flight mass spectrometry (GC × GC-TOFMS). The identified organic compounds have been classified into groups, and quantitative methods were used to calculate their concentrations. Primary emission sources make significant contributions to the atmospheric organic compounds and six groups (including n-alkanes, polycyclic aromatic hydrocarbons (PAHs), levoglucosan, branched-alkanes, n-alkenes and alkyl-benzenes) account for 66% of total identified organic compound mass. In addition, PAHs, and oxygenated PAHs (O-PAHs) were abundant amongst the atmospheric organic compounds on both haze and non-haze days. The most abundant hydrocarbon groups were observed with a carbon atom range of C_{19}-C_{28}. In addition, the total concentration of unidentified compounds present in the chromatogram was estimated in the present study. The total identified compounds account for approximately 47% of total organic compounds ($\geq C_6$) in the chromatogram on both the non-haze and haze days. The total mass concentrations of organic compounds ($\geq C_6$) in the chromatogram were 4.0 μg m^{-3} and 7.4 μg m^{-3} on the non-haze and haze days respectively, accounting for 26.4% and 18.5% of organic matter respectively on those days estimated from the total organic carbon concentration. Ratios of individual compound concentrations between haze and non-haze days do not give a clear indication of the degree of oxidation, but the overall distribution of organic compounds in the chromatogram provides strong evidence that the organic aerosol is less G.C.-volatile and hence more highly oxidised on haze days.

Keywords: Organic aerosol; GC × GC-TOFMS; PAHs; Haze; $PM_{2.5}$ Beijing, China

1. INTRODUCTION

China is suffering from severe $PM_{2.5}$ pollution, especially in its capital, the annual average concentration of $PM_{2.5}$ in Beijing being in the range 69.7~122 μg m^{-3} from 2000 to 2015 (Lang et al., 2017), 2.0~3.5 times the national standard (35 μg m^{-3}). A recent study showed that the average $PM_{2.5}$ concentration during the haze days was 256 μg m^{-3} in the winter period from December 1, 2015 to December 31, 2015 in Beijing, and very much higher than that of non-haze days (24.7 μg m^{-3}) (Li, et al. 2019), and 25 times the World Health Organization (WHO) guideline of 10 μg m^{-3}.

Organic matter is a large and important fraction of atmospheric fine particles, and a substantial number of organic compounds can be found in the atmospheric particulate phase and may originate as either primary emissions or from secondary formation process (Wu et al., 2018). The primary emission tracers and precursor compounds have been extensively studied in the Beijing aerosol and showed significant contributions from coal combustion, biomass burning and traffic emissions (Ren et al., 2016; Yao et al., 2016). These studies concentrated on the identification of individual organic compounds from the organic aerosol, such as n-alkanes, n-alkenes, PAHs and hopanes, but the structurally specific identification of the chemical composition of the organic aerosol is far from complete. Due to its huge complexity, particulate organic matter is still inadequately characterized up to the present. Hence, the identification of organic compounds in generic groups may be more informative in elucidating the molecular distribution of atmospheric organic compounds, and bulk aerosol characteristics (Alam et al., 2018). Previous studies have shown that the organic compounds were highly oxidized during haze days, and secondary formation has made a significant contribution to the PM (Li et al., 2019). However, these studies focused only on specific individual oxidized organic compounds or the ratios of C, N and O to assess the entire aerosol ageing process (Li et al., 2019), and the relationship between the molecular distribution and oxidizing processes during haze formation is still not clear.

Two-dimensional gas chromatography (GC×GC) coupled with TOF-MS offers much enhanced resolution of complex mixtures, and the technique has been extended in the last 10 years to encompass atmospheric analysis. The two independent analytical dimensions in GC×GC-TOF/MS make this technique potentially ideal for measuring the organic components within a complex matrix such as ambient particulate matter (Hamilton et al., 2004; Welthagen et al., 2003), and its ability to separate complex mixtures of organics at low concentrations makes it an ideal technique to measure partially oxidised, isomeric and homologous series compounds and even groups of compounds (Alam et al., 2016a; Alam and Harrison, 2016; Hamilton et al., 2004). In an earlier study of organic compounds in the Beijing atmosphere, Zhou et al. (2009) reported that 68.4% of particulate organic matter was in the previously "unresolved complex mixture" found in conventional GC separations. The GC × GC technique is able to resolve and identify the components contributing to the unresolved mixture, and the molecular distribution of atmospheric organic compounds can be clearly identified in the chromatogram.

In order to establish relationships between organic compounds in fine particles and their characteristics on non-haze and haze days, as well as to identify the relative importance of their emission sources, further investigation of particulate organic matter composition has been conducted. The objective of this study was to investigate the organic compounds with carbon number higher than C_6 in $PM_{2.5}$ samples collected in central Beijing during wintertime, 2016. In this paper, particle samples were analysed by the GC×GC-TOFMS technique after solvent extraction and the detailed organic composition was observed for polar and non-polar organic compound groups. Here, we report a large number of organic compounds, and their concentrations and molecular distributions sampled on non-haze and haze days. The characteristics of the molecular distribution of atmospheric organic compounds on non-haze days were analysed and compared with haze days during aerosol ageing. In addition, we report their possible sources, formation processes, and reveal and assess their pollution characteristics during non-haze and haze periods. Finally,

105 the mass of unidentified organic compounds (>C_6) is estimated and compared between non-haze and
106 haze days.
107
108 ## 2. MATERIALS AND METHODS
109 ### 2.1 Sampling Method and Site Characteristics
110 $PM_{2.5}$ samples were collected at the Institute of Atmospheric Physics (IAP), Chinese Academy of
111 Sciences in Beijing, China. The sampling site (39º58'N, 116 º 22'E) was located between the North 3rd
112 Ring Road and North 4th Ring Road. The site is approximately 1 km from the 3rd Ring Road, 200 m
113 west of the G6 Highway (which runs north-south) and 50 m south of Beitucheng West Road (which runs
114 east-west). The annual average vehicular speeds in the morning and evening traffic peak were 27.4 and
115 24.3 km h^{-1}, respectively. No industrial sources were located in the vicinity of the sampling site. The
116 experimental campaign took place from November 9 to December 11, 2016. The samples were collected
117 onto pre-baked quartz fibre filters (Pallflex) by a gravimetric high volume sampler (Tisch, USA) with a
118 $PM_{2.5}$ inlet at a flow rate of 1.0 m^3 min^{-1} during the sampling period. The collecting time was 24 h per
119 sample and 3 blank samples were collected during this period. The filters were previously enveloped
120 with aluminium foils and then baked at 450 °C for 6 hours before sampling. After sampling, each filter
121 was packed separately and stored in a refrigerator below -20°C until the analysis.
122
123 ### 2.2 Analytical Instrumentation
124 The sample extracts were analyzed using a 2D gas chromatograph (GC, 7890A, Agilent Technologies,
125 Wilmington, DE, USA) equipped with a Zoex ZX2 cryogenic modulator (Houston, TX, USA). The first
126 dimension was separated on a SGE DBX5, non-polar capillary column (30.0 m, 0.25 mm ID, 0.25 mm
127 – 5.00% phenyl polysilphenylene-siloxane), and the second-dimension column was a SGE DBX50 (4.0
128 m, 0.10 mm ID, 0.10 mm – 50.0% phenyl polysilphenylene-siloxane). The GC × GC was interfaced

129 with a Bench-ToF-Select, time-of-flight mass spectrometer (ToF-MS, Markes International, Llantrisant,
130 UK). The acquisition speed was 50.0 Hz with a mass resolution of >1200 fwhm at 70.0 eV and the mass
131 range was 35.0 to 600 m/z. All data produced were processed using GC Image v2.5 (Zoex Corporation,
132 Houston, US).
133
134 **2.3 Extraction and Analysis Methods of Filters**
135 The filters were spiked with 30.0 μL of 30.0 μg mL^{-1} deuterated internal standards (pentadecane-d_{32},
136 eicosane-d_{42}, pentacosane-d_{52}, triacontane-d_{62}, butylbenzene-d_{14}, nonylbenzene-2,3,4,5,6-d_5, biphenyl-
137 d_{10}, p-terphenyl-d_{14}; Sigma-Aldrich, UK) for quantification and then immersed in
138 methanol/dichloromethane (DCM) (1:1, v/v), and ultra-sonicated for 20 min at 20ºC. The extract was
139 filtered using a clean glass pipette column packed with glass wool and anhydrous Na_2SO_4, and
140 concentrated to 100 μL under a gentle flow of nitrogen for analysis using GC × GC-ToF-MS. 1 μL of
141 the extracted sample was injected in a split ratio 50:1 at 300ºC. The initial temperature of the primary
142 oven (80ºC) was held for 2 min and then increased at 2ºC min^{-1} to 210ºC, followed by 1.5 ºC min^{-1} to
143 325ºC. The initial temperature of the secondary oven (120ºC) was held for 2 min and then increased at
144 3ºC min^{-1} to 200ºC, followed by 2ºC min^{-1} to 300ºC and a final increase of 1ºC min^{-1} to 330ºC to ensure
145 all species passed through the column. The transfer line temperature was 330ºC and the ion source
146 temperature was 280ºC. Helium (99.999%) was used as the carrier gas at a constant flow rate of 1 mL
147 min^{-1}. Further details of the instrumentation and data processing methods are given by Alam and
148 Harrison (2016) and Alam et al. (2016a).
149
150 **2.4 Qualitative and Quantitative Analysis**
151 Standards used in these experiments included 26 n-alkanes (C_{11} to C_{36}), EPA's 16 priority pollutant
152 PAHs, 4 hopanes (17α(H),21β(H)-22R-homohopane, 17α(H),21β(H)-hopane, 17b(H),21a(H)-30-

153 norhopane and 17α(H)-22,29,30-trisnorhopane, 7 decalins and tetralines (cis/trans-decalin, tetralin, 5-
154 methyltetraline, 2,2,5,7-tetramethyltetraline, 2,5,8-trimethyltetraline and 1,4-dimethyltetraline), 4
155 alkyl-naphthalenes (1-methyl-naphthalene, 1-ethyl-naphthalene, 1-n-propyl-naphthalene and 1-n-
156 hexyl-naphthalene), 13 alkyl-cyclohexanes (n-heptyl-cyclohexane to n-nonadecyl-cyclohexane), 5
157 alkyl-benzenes (n-butyl-benzene, n-hexyl-benzene, n-octyl-benzene, n-decyl-benzene and n-dodecyl-
158 benzene) (Sigma-Aldrich, UK, purity >99.2%), 11 n-aldehydes (C_8 to C_{13}) (Sigma-Aldrich, UK, purity
159 ≥95.0%), C_{14} to C_{18} (Tokyo Chemical Industry UK Ltd, purity >95.0%); and 11 2-ketones, C_8 to C_{13}
160 and C_{15} to C_{18} (Sigma-Aldrich, UK, purity ⩾98.0%) and C_{14} (Tokyo Chemical Industry UK Ltd, purity
161 97.0%), 4 n-alcohols (2-decanol, 2-dodecanol, 2-hexadecanol and 2-nonadecanol) (Sigma-Aldrich, UK,
162 purity 99.0%) and 1-pentadecanol (Sigma-Aldrich, UK, purity 99.0%).
163
164 Compound identification was based on the GC×GC-TOFMS spectral library, NIST mass spectral
165 library and on co-injection with authentic standards. Compounds within the homologous series for
166 which standards were not available were identified by comparing the retention time interval between
167 homologues, and by comparison of mass spectra with the standards for similar compounds within the
168 series, by comparison to the NIST mass spectral library, and by the analysis of fragmentation patterns.
169 The quantification for identified compounds was performed by the linear regression method using the
170 seven-point calibration curves (0.05, 0.10, 0.25, 0.50, 1.00, 2.00, 3.00 ng μL^{-1}) established between the
171 authentic standards/internal standard concentration ratios and the corresponding peak area ratios. The
172 calibration curves for all target compounds were highly linear (r^2>0.98, from 0.978 to 0.998),
173 demonstrating the consistency and reproducibility of this method. Limits of detection for individual
174 compounds were typically in the range 0.001–0.08 ng m^{-3}. The identified compounds which have no
175 commercial authentic standards were quantified using the calibration curves for similar structure
176 compounds or isomeric compounds. This applicability of quantification of individual compounds using

177 isomers of the same compound functionality (which have authentic standards) has been discussed
178 elsewhere and has a reported uncertainty of 24% (Alam et al., 2018).
179
180 The branched alkanes, alkyl-benzenes, alkyl-decalins, alkyl-phenanthrene and anthracene (alkyl-Phe and
181 Ant), alkyl-naphthalene (alkyl-Nap) and alkyl-benzaldehyde were identified in the samples with the
182 graphics method of the GC Image v2.5 (Zoex Corporation, Houston, US), and the detailed descriptions
183 are given elsewhere (Alam et al., 2018). Briefly, the structurally similar compounds (similar physico-
184 chemical properties) were identified as a group via drawing a polygon around a section of the
185 chromatogram with the polygon selection tool. All compounds included in the polygon belong to a
186 special compound class and the total concentrations were calculated via a calibration curve of the
187 adjacent compounds and internal standards (IS).
188
189 Field and laboratory blanks were routinely analysed to evaluate analytical bias and precision. Blank
190 levels of individual analytes were normally very low and, in most cases, not detectable. The major
191 contaminants observed were very minor amounts of n-alkanes ranging from C_{11} to C_{21}, with no carbon
192 number predominance and maximum at C_{18}; PAH were not detectable. The major proportion of the
193 contaminants could be distinguished by their low concentrations and distribution fingerprints (especially
194 the n-alkanes). These contaminants did not interfere with the recognition or quantification of the
195 compounds of interest. Recovery efficiencies were determined by analysing the blank samples spiked
196 with standard compounds. Mean recoveries ranged between 82 and 98%. All quantities reported here
197 have been corrected according to their recovery efficiencies. Analytical data from the GC×GC analysis
198 were compared with a conventional GC-MS analysis for levoglucosan and 13 PAH. The results from two
199 analytical instruments were compared, and the correlations (r^2) between them were in the range of 0.5 to
200 0.8 with 10 mean concentrations of individual compounds from each technique within 20% of one

another, 2 within 20-30% and the remainder (2) within 30-40% of one another. The largest outlier was levoglucosan, which was underestimated, probably since it decomposed due to a lack of the usual derivatisation.

3. RESULTS AND DISCUSSION

3.1 General Aerosol Characteristics

Thirty-three samples were separated into non-haze (13) and haze (20) days (the latter with $PM_{2.5}$ exceeding 75 μg m^{-3} for 24 h average) according to the National Ambient Air Quality Standards of China (NAAQS) released in 2012 by the Ministry of Environmental Protection (MEP) of the People's Republic of China. The concentrations of $PM_{2.5}$, black carbon (BC), organic carbon (OC), element carbon (EC), gaseous pollutants (SO_2, NO, NO_2, NO_x, and CO) and meteorological parameters (wind speed (WS), wind direction (WD) and relative humidity (RH)) were simultaneously determined during the field campaigns and appear in Table S1.

The average daily $PM_{2.5}$ mass was 99 μg m^{-3}, and haze days (average 141 μg m^{-3}) were four times higher than that of non-haze days (35.3 μg m^{-3}). The wind and temperature during the haze and non-haze days were 0.94 and 1.44 m/s, 6.07 and 4.0°C, respectively. However, the relative humidity during haze episodes (56.3%) was slightly higher than the non-haze periods (39.8%). The concentrations of gaseous pollutants SO_x, NO_x, and CO were simultaneously elevated with the increase of $PM_{2.5}$ concentrations, whereas the O_3 concentration presented an opposite trend to $PM_{2.5}$ concentrations (Lyu et al., 2019). The average concentration of organic matter (OM) was estimated as 30.2 μg m^{-3} using the OC concentration (18.9 μg m^{-3}) and a multiplying factor of 1.6 for aged aerosols (Turpin and Lim, 2001). The OM concentration was 40.0 μg m^{-3} and 15.0 μg m^{-3} on haze and non-haze days respectively.

3.2 The Major Classes of Organic Compounds in $PM_{2.5}$

More than 6000 peaks were found in the 2D chromatogram image of each sample by the data processing software (GC Image v2.5). Over 300 polar and non-polar organic compounds (POCs and N-POCs) were identified and quantified in the $PM_{2.5}$ samples, and these compounds are grouped into more than twenty classes, including normal and branched alkanes, n-alkenes, aliphatic carbonyl compounds (1-alkanals, n-alkan-2-ones and n-alkan-3-ones), n-alkanoic acids, n-alkanols, PAHs, oxygenated PAHs (OPAHs), alkylated-PAHs, hopanes, alkyls-benzenes, alkyl-cyclohexanes, pyridines, quinolines, furanones, and biomarkers (levoglucosan, cedrol, phytane, pristane, supraene and phytone). The details of aliphatic hydrocarbon measurements (including n-alkanes, n-alkenes) and carbonyl compounds (including n-alkanals, n-alkan-2-ones, n-alkan-3-ones, furanones and phytone) have been reported in previous articles (Lyu et al. 2018a,b). The total concentrations of identified organic compounds ranged from 0.94 to 5.14 μg m^{-3} with the average of 2.84 ± 1.19 μg m^{-3}, accounting for 9.40 % of OM. The concentrations of identified individual organic compounds are summarized in Table S2, and the percentage of each group in the total identified organic compounds is in Figure 1. The n-alkanes (16%) make the greatest contribution to the total mass of identified organic compounds, followed by levoglucosan (13%), branched-alkanes (13%), PAHs (10%), n-alkenes (7%) and alkyl-benzenes (7%). These six groups account for 66% of total identified organic compounds by mass, and a total concentration of 1.41 μg m^{-3}, accounting for 1.42% of the particle mass. In a study in Nanjing, Haque et al. (2019) reported the most abundant classes of organic compounds to be n-alkanes (205 ng m^{-3}), followed by fatty acids (76.3 ng m^{-3}), PAHs (64.3 ng m^{-3}), anhydrosugars (levoglucosan, galactosan and mannosan, 56.3 ng m^{-3}), fatty alcohols (40.5 ng m^{-3}) and phthalate esters (15.2 ng m^{-3}).

3.3 The Characteristics of Organic Compound Groups on Non-haze and Haze Days

The average total concentration of identified groups was calculated for the non-haze (13 days) and haze periods (20 days). The comparisons of two periods (non-haze and haze days) are shown in Figure 2, and the detailed concentrations of each group are shown in the Table S3. The concentrations of most organic compound groups on the haze days were higher than non-haze days, especially for the n-alkanols and n-Cn-cyclohexanes. The alkyl-benzenes, alkyl-benzaldehydes, monoaromatic compounds and quinoline have approximately similar concentrations on the non-haze and haze days.

As many compound groups have not been reported in previous studies, and complete data on the relative abundance of these compounds in various source emissions are not available at present, it is not yet possible to calculate source contributions to ambient organic compound concentrations via molecular marker or mathematical modelling methods. However, several important consistency checks on the potential source can be performed. In the sections that follow, the literature on the origin of each of these compound classes is reviewed briefly and the measured compound concentrations are described. Table 1 shows the comparison of identified organic compounds between the present and previous studies in Beijing. In many, but not all cases, concentrations are comparable.

3.3.1 n-Alkanoic acids, n-alkanols and carbonyl compounds

The n-alkanoic acids with carbon numbers from C_6 to C_{10} were identified in the $PM_{2.5}$. Higher molecular weight alkanoic acids generated from the biomass burning (Simoneit and Mazurek, 1982) were not identified from the samples probably due to low volatility in the G.C. The n-alkanoic acids were observed at a similar magnitude to a previous study in Beijing (Zhou et al., 2009) (Table 1).

Previous studies have found that the n-alkanoic acid homologues were significantly impacted by cooking

emissions in Beijing and showed higher concentrations on non-haze days and a similar distribution pattern in all seasons (Huang et al., 2006; He et al., 2006b; Sun et al. 2013). Consistent results for acids were observed in this study, and the ∑ n-alkanoic acids had an average concentration on the non-haze days with an average concentration of 36.4 ng m^{-3}, higher than 24.6 ng m^{-3} on haze days, strongly implying a dominant contribution from cooking emissions as opposed to secondary formation.

In the present study, 1-alkanols with even-carbon numbers from C_{12} to C_{20} were identified in the $PM_{2.5}$, with a quite similar molecular distribution to that of diesel engine exhaust samples (Alam et al., 2016b). In addition, other primary emission sources may make a potential contribution to these compounds, including from biomass burning (Zhang et al., 2007). The average ∑ n-alkanols concentration was 38.5 ng m^{-3}, and ∑ n-alkanols had higher concentrations on the haze days (59.8 ng m^{-3}), approximately eight times greater than 8.39 ng m^{-3} on non-haze days. The above results suggest that n-alkanol formation is more efficient on haze days, even though vehicular emissions appear to be another important source.

Aliphatic carbonyl compounds including n-alkanals, n-alkan-2-ones and n-alkan-3-ones, have been described in detail by Lyu et al. (2019). Briefly, the daily sum of aliphatic carbonyls (ΣAC), ranged from 8.87 to 164 ng m^{-3}, accounting for 0.02–0.46% of OM. The average ΣAC was 75.8 ng m^{-3} during all haze days, approximately double the 39.5 ng m^{-3} of the non-haze period. Lyu et al. (2019) showed that the n-alkanals were mainly originated from vehicle exhaust or formed from OH oxidation of n-alkanes, while the n-alkanones were probably emitted mainly by coal combustion.

3.3.2 Nitrogen-containing organic compounds (N-CC)

Nitrogen-containing (N-containing) organic compounds have been reported in many previous studies, and the important sources of N-containing compounds are coal combustion, biomass burning, vehicular

exhaust and atmospheric photochemical reactions (Rogge et al., 1994; Rogge et al., 1993b; Schauer et al., 1996; Zhang et al., 2002; Zhang et al. 2002; Fan et al. 2018). N-containing compounds were identified in the samples, including heterocyclic compounds (alkyl-pyridines, alkyl-quinolines) and other N-containing compounds (nitro, amine compounds). The average Σ alkyl-pyridines, Σ alkyl-quinolines and Σ other N-containing compounds were 17.4 ± 7.58, 16.6 ± 15.0 and 30.0 ± 23.1 ng m^{-3}, respectively, and the average total concentrations of N-containing compounds was 64.0 ng m^{-3}, accounting for approximately 0.2% of the OM.

The quinolines have been proposed for use as tracers of vehicular exhaust (Rogge et al., 1993a) and crude oils and shale oil combustions (Schmitter et al., 1983; Simoneit et al., 1971), while the straight chain alkyl-pyridines (n-Cn-pyridine) are related to petrochemical industries (Botalova et al., 2009) and secondary formation from pyrolysis of proteins and amino acids under a high temperature (Chiavari and Galletti, 1992; Hendricker and Voorhees, 1998; Kögel-Knabner, 1997). This study found that both quinolines and alkyl-pyridines showed similar concentrations on the non-haze and haze days, 16.8 ± 16.5 ng m^{-3} (non-haze) and 16.5 ± 14.4 ng m^{-3} (haze days) and 12.0 ± 6.02 ng m^{-3} (non-haze days) and 15.3 ± 8.36 ng m^{-3} (haze days) respectively. Amino compounds can originate form biomass burning and coal combustion, and are abundant in winter fine particulate matter samples compared to summer (Zhang et al., 2002; Akyiiz 2008). In the present study, the average ∑other N-containing compounds was 34.2 ± 24.6 ng m^{-3} on the haze days, somewhat higher than 22.6 ± 19.4 ng m^{-3} on non-haze days.

The similar concentrations on the non-haze and haze days suggests that N-containing organic compounds mainly originated from primary sources and subject to degradation during the haze formation process.

Tracers of tobacco smoke, benzoquinoline and isoquinoline have previously been determined in the PM

collected in Beijing, with concentrations of 3.10 and 0.22 ng m^{-3} respectively (Zhou et al., 2009). These two compounds were also identified in the present study, with 4.40 and 0.80 ng m^{-3}, respectively. Phthalimide was identified in the PM at 0.91 ng m^{-3}, and was considered to be derived from cyclization and aromatization reactions of proteins or from intermediates in the transformation of carboxyl ammonium salts to nitriles by Zhao et al. (2009).

3.3.3 Esters

Phthalate esters are organic chemicals that are commonly used in a variety of consumer products and in various industrial and medical applications, and are predominantly used as plasticizers to improve the flexibility of polyvinyl chloride (PVC) resins and other polymers. Table 1 shows a comparison of phthalate esters (DBP, DEP, DEHP) between the present and previous studies in the winter in Beijing; it seems that the concentrations of some phthalate esters have significantly decreased from earlier studies (Wang et al., 2006; Zhou et al., 2009). The present study found that diisodecyl phthalates, DBP and DEHP were abundant compounds in the ester group with 49.7 ± 43.2, 16.9 ± 15.5 and 16.0 ± 12.6 ng m^{-3}, respectively. The DBP, DEP and DEHP in Beijing were far lower than that in winter in Tianjin (Kong et al., 2013) and another fifteen cities around China (Li and Wang, 2015; Wang and Kawamura, 2005; Wang et al., 2006). In addition, the average ∑ Ester was 117 ± 82.1 ng m^{-3}, with 132 ± 87.1 and 89.4 ± 70.0 ng m^{-3} on haze and non-haze days, respectively. Since phthalates are not chemically bound to the polymeric matrix, they can enter the environment by escaping from manufacturing processes and by leaching or vaporising from final products (Staples et al., 1997).

3.3.4 PAHs, O-PAHs and alkylated-(PAHs & OPAHs)

In all, 23 PAHs (2-6 rings), 19 oxygenated PAHs (O-PAHs) and 14 alkylated-(PAHs & OPAHs) were determined in the $PM_{2.5}$ samples. The average total polycyclic aromatic compounds (the sum of ∑ PAHs,

343 ∑ O-PAHs, ∑alkylated-(PAHs & OPAHs), alkyl-PHE and ANT and alkyl-NAP) was 569 ng m^{-3},
344 accounting for 1.88 % of OM.
345
346 The distribution of PAHs is shown in Figure 3; the most abundant PAHs were BbF, followed by CHR,
347 FLT, BaA and PYR. In all samples, the ∑ PAHs ranged from 46.7-727 ng m^{-3} with average 281 ± 176
348 ng m^{-3}, accounting for 0.93 % of OM. In addition, the average ∑ PAHs was 364 ng m^{-3} during haze days,
349 but only 159 ng m^{-3} on the non-haze days. It should be noted that retene was detected in most samples,
350 with an average concentration of 14.4 ± 17.5 ng m^{-3}. It has been suggested that retene predominantly
351 originates from the combustion of conifer wood (Simoneit et al., 1991).
352
353 Nineteen oxygenated PAHs (O-PAHs) make up of a class of PAH derivatives that are present in the
354 atmosphere as a result of direct emission during combustion and secondary formation by homogeneous
355 and heterogeneous photo-oxidation processes (Keyte et al., 2013; Ringuet et al., 2012). They are also of
356 scientific interest because they are, typically, found in the secondary organic aerosol (SOA) formed by
357 photo-oxidation of PAH (Shakya and Griffin, 2010). In urban samples, polycyclic aromatic ketones
358 (PAK), polycyclic aromatic quinones (PAQ) and polycyclic aromatic furanones (PAF) are typical groups
359 of compounds (Lin et al., 2015). The average total concentrations of O-PAH measured in this study
360 (Figure 4) was 67.9 ng m^{-3}. The polycyclic aromatic ketones 4,5-pyrenequinone (4,5-PyrQ) (8.75 ng m^{-3})
361 and 1,6-pyrenequinone (1,6-PyrQ) (7.38 ng m^{-3}) were the most abundant compounds during the
362 sampling campaign. Four O-PAHs have been identified previously at the PKU site in the 2012 heating
363 season in Beijing (Table 1); it is notable that the concentration of AQ was up to 108 ng m^{-3},
364 approximately 20 times that in the present study (5.12 ng m^{-3}). As O-PAHs can be formed during
365 sampling, it is necessary to be very careful in reconciling their presence with specific sources (Pitts et al.,
366 1980). The average ∑ O-PAHs was 86.5 ng m^{-3} during haze days, but 39.7 ng m^{-3} on the non-haze days.

The ratio of quinone: parent PAH has been used to assess the air mass age (Alam et al., 2014; Harrison et al., 2016). The average ratios of phenanthraquinone to phenanthrene (PQ:PHE), anthraquinone to anthracene (AQ:ANT) and benzo(a)anthracene-7,12-quinone to benzo(a)anthracene (BaAQ:BaA) were 0.37, 1.27, 0.32, respectively, with PQ:PHE, AQ:ANT and BaAQ:BaA ratios of 0.25, 0.88 and 0.26 on the haze days, which were lower than 0.55, 1.92, 0.40 on non-haze days. The BaAQ:BaA ratios were lower than earlier published data of 1.28 measured in Beijing (Li et al., 2019), 1.40 in Xian (Wang et al., 2016) and 0.54 in Beijing-Tianjing (Wang, 2010), but higher than the 0.08 measured in Guangzhou (Wei et al., 2012) and 0.09 in Zhuanghu (Ding et al., 2012). Shen et al. (2011) reported that the BaAQ:BaA ratio was 0.03 for coal combustion, 0.16 for crop residue burning (Shen et al., 2012a) and 6.6 from biomass pellet burning (Shen et al., 2012b). The low ratios of O-PAHs/PAHs in our data probably indicated that the particulate matter mainly originated from coal combustion and biomass burning. However, the lower ratios on haze days than non-haze days may imply continued oxidation of the O-PAH to products which were not analysed. Li et al. (2019) also reported that ratios of ΣOPAH to ΣPAH were very similar during haze and clean air periods, which provides support for this conclusion.

3.3.5 Molecular markers

The hopanes are compounds present in crude oil as a result of the decomposition of sterols and other biomass and are not by-products of combustion (Simoneit, 1985). They are very stable and have been proposed for use as tracers for atmospheric particles from fossil fuel combustion, such as motor vehicle exhaust (Simoneit, 1985) and coal combustion (Oros and Simoneit, 2000). The hopanes are widely used as tracers of traffic emission due to vehicle emissions having high loadings of hopanes (Cass, 1998). The comparison of hopanes between this study and previous studies in the winter or heating season of Beijing are shown in Table 1. Hopanes were extensively present in Beijing $PM_{2.5}$ samples, and their carbon numbers ranged from C_{27} to C_{32}, but not C_{28} (Table 2). The average concentration of hopanes in Beijing

was 32.7 ± 24.7 ng m^{-3}, with 15.2 ± 10.7 ng m^{-3} and 44.6 ± 24.6 ng m^{-3} on non-haze and haze days, respectively. Previous studies have found that C_{29} (17a(H), 21h(H)-norhopane) was dominant in the hopane series and consistent with that from coal combustion (He et al., 2006a), while C_{30} (17β(H)21α(H)-hopane and 17a(H), 21β(H)-hopane) was similar to C_{29} in the winter time in Beijing and attributed to gasoline and diesel exhaust (Simoneit, 1985).

Levoglucosan and methoxyphenols from pyrolysis of cellulose and lignin are usually used as unique tracers for biomass burning in source apportionment models (Schauer and Cass, 2000). Levoglucosan (1,6-anhydro-β-D-glucopyranose) has been for a long time employed as the specific molecular marker for long-range transport of biomass burning aerosol, based on its high emission factors and assumed chemical stability (Fraser and Lakshmanan, 2000; Simoneit et al., 2000). It is a highly abundant compound and the concentrations in winter in Beijing have a significant fluctuation (Table 1). The average ∑ levoglucosan was 355 ± 232 ng m^{-3} during the entire sampling period, and 417 ± 223 ng m^{-3} in haze episodes, approximately twofold that of the non-haze days, 238 ± 193 ng m^{-3}, indicating a significant impact of biomass burning upon wintertime aerosols in Beijing.

Methoxyphenols are usually also considered as tracers for wood burning (Simpson et al., 2005; Yee et al., 2013) with the average ∑ Methoxyphenols 7.29 ± 7.11 ng m^{-3}, and the haze days (9.03 ± 7.93 ng m^{-3}) twofold greater than non-haze days (4.74 ± 4.95 ng m^{-3}) during the campaigns. In Beijing and its surrounding areas, harvest occurs in late September to October for corn, and biomass fuels are used for cooking and heating purpose in the winter. However, the methoxyphenols are abundant components in the smoke from broad-leaf tree and shrub burning (Wang et al., 2009), and have been identified in all coal smoke (Simoneit, 2002a), so cannot be used as source-specific markers for biomass burning.

Phenolic compounds from the thermal degradation of lignin have been proposed as potentially useful tracers for wood smoke, and many of them are emitted in relatively high quantities and are specific to wood combustion sources (Simoneit, 2002b; Simoneit et al., 2004). Another important source of phenolic compounds is oxidation of monoaromatic compounds and PAHs (Pan and Wang, 2014). Phenols and naphthalenol were identified in the $PM_{2.5}$, with the average $\sum$ phenolic compounds 21.6 ± 17.0 ng m^{-3}, with 14.0 ± 13.2 ng m^{-3} and 25.9 ± 17.9 ng m^{-3} on the non-haze and haze days, respectively. However, it is notable that the concentrations of naphthalenol identified in the present study were far lower than that of previous studies (Table 1).

Pristane (Pr) and phytane (Ph) have been found in the exhaust of petrol and diesel engines and in lubricating oil, indicating their origin from petroleum (Simoneit, 1984). Since their presence is ubiquitous in vehicle exhausts and negligible in contemporary biogenic sources in urban environments, they can be used as petroleum tracers for airborne particulate matter. The mean values of Pr and Ph in our samples are 2.24 and 1.94 ng m^{-3}, respectively. Biogenic inputs are often characterised by a predominance of the odd carbon alkanes and Pr. Since Ph is rarely found in biological material, most biological hydrocarbons have a Pr/Ph ratio far higher than 1.0 (Oliveira et al., 2007), but values approaching unity indicate a hydrocarbon signature derived from petrochemical use. The average Pr/Ph ratios were 1.15 for $PM_{2.5}$ samples, and this finding is quite similar to the results from the southern Chinese city of Guangzhou, 1.1-1.8 (Bi et al., 2002), but almost four times greater than Beijing summer samples (0.3) (Simoneit et al., 1991). The high Pr/Ph indicated that the hydrocarbons in urban aerosol derive mainly from petroleum residues probably deriving from vehicular emissions in Beijing.

3.4 The Molecular Distributions of Aliphatic Hydrocarbons

Figure 4 shows the molecular distributions of aliphatic hydrocarbons on non-haze and haze days. The

details on the n-alkanes are given by Lyu et al. (2019). Briefly, the Σ n-alkanes (C_{10}-C_{36}) ranged from 42.4 to 1241 ng m^{-3} with an average 450 ± 316 ng m^{-3}, and the average Σ n-alkanes was 577 ng m^{-3} during haze episodes, more than twice that of the non-haze period (264 ng m^{-3}). The n-alkanes (C_{20}-C_{31}) were the most abundant homologues (Figure 4), accounting for approximately 83% of the Σn-alkanes.

The total concentrations of branched alkanes (C_{12}-C_{36}) ranged from 125-647 ng m^{-3} with the average 356 ± 173 ng m^{-3} during the sampling period. The average branched alkanes concentration was 440 ± 144 ng m^{-3} during all haze episodes, which was higher than 234 ± 138 ng m^{-3} on the non-haze days. The most abundant branched alkanes were observed at C_{22}, with the average concentration of 29.2 ng m^{-3}, and the greatest abundance of branched alkanes groups was observed within the carbon atom range of C_{20}-C_{30}, accounting for 67.7% of Σ branched alkanes. The branched alkanes have lower concentrations than n-alkanes when the carbon number is >C_{20} on haze and non-haze days, while showing higher concentrations than n-alkanes when the carbon number is lower than C_{19}.

It is difficult to identify the potential sources of branched alkanes from the literature, although Alam et al. (2016b) reported that branched alkanes (C_{11}-C_{33}) were an abundant compound group in diesel exhaust. The increase of high molecular weight branched alkanes (C_{20}-C_{30}) from non-haze days to haze days is consistent with a primary emission source, probably linked to coal combustion or vehicular emissions. The fact that both n-alkanes and branched alkanes increase quite similarly between non-haze and haze conditions is consistent with them arising from the same source(s), or sources with highly correlated emissions.

Other groups of aliphatic and alicyclic compounds identified in the $PM_{2.5}$, include alkyl-decalins, alkyl-pyridines, alkyl-furanones, alkyl-cyclohexanes and alkyl-benzenes. Figure 5 shows the molecular

distributions of these series of compounds. Engine studies (Alam et al., 2016b) have also found that compounds observed in vehicle exhaust beside n-alkanes and PAHs, include straight and branched cyclohexanes (C_{11}-C_{25}), various cyclic aromatics, alkyl-decalins and alkyl-benzenes. The particle-bound n-Cn-cyclohexanes with carbon numbers from C_{12} to C_{26} were identified in diesel exhaust (Alam et al., 2016b) with a dominant range C_{18}-C_{25}, and the total (particle + gas) concentration of n-C_n-cyclohexanes was 2.05 μg m^{-3}. The n-Cn-cyclohexanes (C_{20}-C_{30}) were identified at the IAP site with average ∑ n-C_n-cyclohexane 39.4 ± 37.1 ng m^{-3}. The most abundant range was observed at C_{22}-C_{27}, highly consistent with the engine study, implying a significant contribution from vehicle emissions. In addition, the average Σn-C_n-cyclohexane (C_{20}-C_{30}) was 53.3 ± 39.3 ng m^{-3} during haze episodes, approximately five times higher than 10.8 ± 8.22 ng m^{-3} in the non-haze period, a larger ratio than for other primary emissions. The alkyl-decalins and tetralin are products obtained by hydrogenation of naphthalene and its derivatives during the refining process and have been identified in vehicle exhaust (Afzal et al., 2008; Alam et al., 2016b; Ogawa et al., 2007). The average ∑ alkyl-decalins was 110 ng m^{-3}, with 85.4 ± 65.5 and 126 ± 110 ng m^{-3} on non-haze and haze days respectively. The Σ n-C_n-benzene (C_{16}-C_{25}) identified in the samples ranged from 7.71 to 410 ng m^{-3} with an average of 56.6 ± 73.0 ng m^{-3}. The average Σ n-C_n-benzene (C_{16}-C_{25}) was 77.2 ± 88.2 ng m^{-3} during haze episodes, approximately four times the 23.3 ± 15.1 ng m^{-3} of the non-haze period. Other alkyl-benzenes (C_9-C_{25}) were also identified and have higher concentrations at C_{12}, especially for the non-haze days.

3.5 Distribution of Compounds with respect to Volatility and Polarity, and the Estimation of Unidentified Mass

The method for characterising the volatility/polarity distribution of compounds is detailed in the Supporting Information. Briefly, the chromatography image was separated into seven parts according to the main chemical and physical properties of the organic compounds and the distribution of internal

standards (IS), and the detailed protocol is shown in Table S4. The diagram of the separated image with seven parts is shown in Figure 6a, and the concentrations measured in each part are shown in Figure 6 and Table 3. In the chromatogram (Figure 6), volatility decreases from left to right and polarity increases from bottom to top. Table 3 shows the estimated mass concentration of all components of the chromatogram, alongside the amount of mass not accounted for by the specific compounds reported in this paper.

For the non-haze days, the sum of identified organic compounds (IOC) with carbon numbers higher than C_6 was 1.84 μg m^{-3}, accounting for 46.5 % of total organic compounds. The IOC of the haze days was almost two times that of non-haze periods, with an average of 3.42 μg m^{-3}, accounting for 46.3% of total measured organic matter. In addition, the sum of unidentified compounds increased from 2.12 μg m^{-3} on non-haze days to 3.96 μg m^{-3} on haze days, accounting for 53.5 % and 53.7% of total measured organic matter, respectively. Hence there is no marked difference in the proportions of identified and unidentified compounds between haze and non-haze conditions.

For the non-haze days, Section 1 of the chromatogram has the highest concentration of 802 ng m^{-3}, followed by Section 7 (792 ng m^{-3}), accounting for 20.3 % and 20.0 % of the total organic compounds respectively, implying that both low molecular weight (LMW) hydrocarbons (Section 1) and high molecular weight (HMW) PAHs (Section 7, 3~6 rings) and compounds of similar volatility/polarity were the main organic components of atmospheric particulate matter measureable by the GCxGC separation technique. The PAHs are important organic compounds appearing in Sections 6 + 7, accounting for 32.3% of total measured organic compounds during the non-haze days. Sections 2, 3 and 4 showed relatively low concentrations, and medium molecular weight hydrocarbons in the range of C_{23}~C_{27} (Section 3) were the more abundant aliphatic hydrocarbons relative to Section 2 (C_{17}~C_{23}) and Section 4 (>C_{27}), probably

caused by primary emissions from vehicular and coal combustion (Cao et al., 2018). Section 5 contains oxidized monoaromatic compounds, and the concentrations were higher than Section 6 (mainly containing naphthalene derivatives) and lower than Section 1, probably mainly arising from vehicular emissions or oxidized from the monoaromatic precursors (Section 1) (Schwantes et al., 2017).

The polarity distribution characteristics of atmospheric organic compounds on the non-haze days were also studied. For the volatile areas, low polarity compounds (Section 1) have a lower concentration than polar compounds (Sections 5 + 6) during the non-haze days. On the contrary, for the semi-and non-volatile area, the sum of low polar compounds (Sections 2 + 3 + 4) have higher concentrations than polar organic compounds (Section 7).

The concentrations in all sections increased from non-haze to haze days, and the main difference between haze and non-haze days attaches to Sections 5, 6 and 7 (Figure 6b), indicating a more polar aerosol during periods of haze. Section 6 has the highest concentrations on the haze days (1556 ng m^{-3}), increased more than three times on the haze days in contrast to non-haze days (485 ng m^{-3}), followed by Section 7 (1337 ng m^{-3}) and Section 5 (1309 ng m^{-3}), indicating that the oxidized monoaromatics, naphthalene derivatives and oxidized HMW PAHs were the main identified components of the atmospheric particulate matter during the haze days. The concentrations were compared among the seven sections, and the highest concentrations of Section 6 were probably contributed by the degradation of HMW PAHs (from Section 7). For the oxidized monoaromatic compounds (Section 5), the degradation of naphthalene derivatives was probably a major contributor, but not compounds oxidized from Section 1. The concentrations of Section 3 were also observed to increase from non-haze days (573 ng m^{-3}) to haze days (1060 ng m^{-3}), indicating that accumulation has an obvious effect on the stable compounds with carbon number between C_{23} to C_{27} during haze formation under low wind speed (Table S1).

3.6 Elevation of Primary and Secondary Constituents during Haze Events

By definition, concentrations of $PM_{2.5}$ are elevated during haze events, but the question arises as to whether primary or secondary organic compounds make a larger contribution to the rise in concentrations. Constituents that are expected to be primary are typically elevated in mean concentration by a factor of around two (Table S3). Examples are n-alkanes (ratio of haze : non-haze of 2.2), levoglucosan (1.8) and hopanes (2.9). This is consistent with the ratios for primary gaseous emissions, including SO_2 (ratio of 2.6), CO (2.5) and NO_x (2.2) (Table S1). Surprisingly, however, both BC (ratio of 3.8) and EC (3.4) (Table S1) are primary constituents with a large haze:non-haze ratio, comparable to that of $PM_{2.5}$ mass (4.0). Consequently the factors leading to an elevation of concentrations during the haze appear complex and are likely to be resolved fully only by chemistry-transport models.

OC/EC ratios are used to estimate the relative contribution of primary and secondary sources; high OC/EC ratios (> 2.0) have been observed for aerosols with significant SOA contributions in Beijing (Lv et al., 2019; Ji et al., 2018). The OC/EC ratio in this study was 3.88 on average, suggesting a significant contribution of SOA in Beijing aerosols, which is consistent with the results of Section 3.5. The aliphatic carbonyls, which have both primary and secondary sources (Lyu et al., 2018a,b) range from ratios of 1.6 (n-alkanals) to 2.8 (n-alkan-2-ones). This result was consistent with Section 3.5; it was found that the chromatogram Sections 2 and 3 which contained alkanals ($C_{15} \leq Cn \leq C_{25}$) and alkanones ($C_{15} \leq Cn \leq C_{25}$) have slighly higher concentrations on haze days than non-haze days. However, the low ratio alkanal and alkanone compounds are quite readily oxidised (Chacon-Madrid et al., 2010; Chacon-Madrid and Donahue, 2011), and a low ratio may reflect a high degree of further processing to form more oxidised species on the haze days compensating for enhanced formation.

There are no compounds in Table S3 certain to be exclusively secondary. However, the results in Figure

6 show an appreciable elevation in more polar compounds (upper part of the chromatogram) on haze days, suggestive of a greater relative abundance of more oxidised, possibly secondary compounds in the haze. The ratio of average $PM_{2.5}$ mass between haze and non-haze days was 4.0, and organic carbon, 2.7 (Table S1). The ratio for organic matter would be greater than 2.7, due to a higher OM/OC ratio in secondary compounds. This is strongly suggestive of a greater contribution from an elevation in secondary than primary species concentrations during the haze events, and that much of the mass lies outside of the chromatogram due to the low volatility of the secondary species.

4. CONCLUSIONS

Over 300 polar and non-polar organic compounds were determined in the fine particle samples from Beijing, and these compounds have been grouped into more than twenty classes, including normal and branched alkanes, n-alkenes, aliphatic carbonyl compounds (1-alkanals, n-alkan-2-ones and n-alkan-3-ones), n-alkanoic acids, n-alkanols, PAHs, oxygenated PAHs (O-PAHs), alkylated-(PAHs & OPAHs), hopanes, n-C_n-benzene, alkyls-benzenes, n-C_n-cyclohexane, pyridines, quinolines, furanones, and biomarkers (levoglucosan, cedrol, phytane, pristane, supraene and phytone). The total concentrations of identified organic compounds ranged from 0.94 to 5.14 μg m^{-3} with an average of 2.84 ± 1.19 μg m^{-3}, accounting for 9.40 % of OM mass. The six groups which accounted for 66% of total identified organic compound mass included n-alkanes, levoglucosan, branched-alkanes, PAHs, n-alkenes and alkyl-benzenes, and these were significantly impacted by primary emission sources. In addition, the average total polycyclic aromatic compounds (the sum of ∑ PAHs, ∑ O-PAHs, ∑alkylated-(PAHs & OPAHs), alkyl-PHE and ANT and alkyl-NAP) was 560 ng m^{-3}, accounting for 1.88 % of OM. The comparisons of identified groups between non-haze and haze periods showed that most organic compound groups have a higher concentration on the haze days relative to the non-haze days. The average sum of the identified compounds increased from 1.84 μg m^{-3} to 3.42 μg m^{-3} from non-haze days to haze days. A

584 unimodal molecular distribution of alkanes was observed in the range from C_8 to C_{36}, and these
585 compounds make significant contributions to atmospheric organic compounds in the range of C_{19}-C_{28},
586 especially on the haze days. The unidentified compounds in the chromatogram were estimated, and the
587 results show that the average sum of unidentified compounds increased from 2.12 μg m^{-3} on non-haze
588 days to 3.96 μg m^{-3} on haze days, accounting approximately for 53.5 % and 53.7% of total organic
589 compounds, respectively. Finally, the total mass concentrations of measured organic compounds (≥C6)
590 was 3.96 μg m^{-3} and 7.39 μg m^{-3} on the non-haze and haze days, accounting for 26.4% and 18.5% of OM
591 mass, respectively on these days. The remaining mass is that which is not volatile under the conditions
592 of the gas chromatography. The higher percentage of non-GC-volatile organic matter on haze days is
593 indicative of a greater degree of oxidation of the organic aerosol, consistent with the difference in the
594 chromatogram between haze and non-haze days. The greater contribution of secondary constituents
595 during haze events has been reported previously by Huang et al. (2014) and Ma et al. (2017), but not the
596 greater extent of oxidation of organic matter. In a modelling study, Li et al. (2017) found that during
597 winter haze conditions in Beijing the majority of secondary $PM_{2.5}$ had formed one or more days prior to
598 arrival, hence explaining its highly oxidised condition.
599
600 **DATA ACCESSIBILITY**
601 Data supporting this publication are openly available from the UBIRA eData repository at
602 https://doi.org/10.25500/edata.bham.00000303.
603
604 **AUTHOR CONTRIBUTIONS**
605 The study was conceived by RMH and ZS and the fieldwork was organised and supervised by ZS and
606 PF. TV and DL undertook air sampling work and general data analyses for the campaign while RL
607 carried analytical work on the Beijing samples under the guidance of MSA and CS. XW contributed

analyses of data from London. RL produced the first draft of the manuscript with guidance from YF and RMH and all authors contributed to the refinement of the submitted manuscript.

ACKNOWLEDGEMENTS

Primary collection of samples took place during the APHH project in which our work was funded by the Natural Environment Research Council (NERC) (NE/N007190/1). The authors would also like to thank the China Scholarship Council (CSC) for support to R.L.

COMPETING INTERESTS

The authors have no conflict of interest.

REFERENCES

Afzal, A., Chelme-Ayala, P., El-Din, A. G., El-Din, M. G.: Automotive Wastes, Water Environ., Res., 80, 1397-1415, 2008.

Akyüz, M.: Simultaneous determination of aliphatic and aromatic amines in ambient air and airborne particulate matters by gas chromatography-mass spectrometry, Atmos. Environ., 42, 3809-3819, 2008.

Alam, M. S., Zeraati-Rezaei, S., Liang, Z., Stark, C., Xu, H., MacKenzie, A. R., Harrison, R. M.: Mapping and quantifying isomer sets of hydrocarbons (≥ C 12) in diesel exhaust, lubricating oil and diesel fuel samples using GC× GC-ToF-MS, Atmos. Meas. Tech., 11, 3047, 2018.

Alam, M. S., Stark, C., Harrison, R. M.: Using variable ionisation energy time-of-flight mass spectrometry with comprehensive GC×GC to identify isomeric species, Anal. Chem., 88, 4211-4220, 2016a.

Alam, M. S., Zeraati-Rezaei, S., Stark, C. P., Liang, Z., Xu, H., Harrison, R. M.: The characterisation of diesel exhaust particles - composition, size distribution and partitioning, Faraday. Discuss., 189, 69-84, 2016b.

Alam, M. S., Harrison R. M.: Recent advances in the application of 2-dimensional gas chromatography with soft and hard ionisation time-of-flight mass spectrometry in environmental analysis, Chem. Sci., 7, 3968-3977, 2016.

Alam, M., Delgado-Saborit, J. M., Stark, C., Harrison, R. M.: Investigating PAH relative reactivity using congener profiles, quinone measurements and back trajectories, Atmos. Chem.Phys., 14, 2467-2477, 2014.

Bi, X., Sheng, G., Peng, P.A., Zhang, Z., Fu, J.: Extractable organic matter in PM_{10} from LiWan District of Guangzhou City, PR China, Sci. Tot. Environ., 300, 213-228, 2002.

Botalova, O., Schwarzbauer, J., Frauenrath, T., and Dsikowitzky, L.: Identification and chemical characterization of specific organic constituents of petrochemical effluents, Water Res., 43, 3797-3812, 2009.

Cao, R., Zhang, H., Geng, N., Fu, Q., Teng, M., Zou, L., Gao, Y., and Chen, J.: Diurnal variations of atmospheric polycyclic aromatic hydrocarbons (PAHs) during three sequent winter haze episodes in Beijing, China, Sci. Tot. Environ., 625, 1486-1493, 2018.

Cass, G. R.: Organic molecular tracers for particulate air pollution sources. TrAC Trends Anal. Chem., 17, 356-366, 1998.

Chacon-Madrid, H. J., and Donahue, N.: Fragmentation vs. functionalization: chemical aging and organic aerosol formation, Atoms. Chem. Phys., 11,10553-10563, 2011.

Chacon-Madrid, H. J., Presto, A. A., and Donahue, N. M.: Functionalization vs. fragmentation: n-aldehyde oxidation mechanisms and secondary organic aerosol formation, Phys. Chem. Chem. Phys., 12, 13975-13982, 2010.

Chiavari, G., Galletti, G. C.: Pyrolysis - gas chromatography/mass spectrometry of amino acids, J.Anal.Appl. Pyrol., 24, 123-137, 1992.

Ding, J., Zhong, J., Yang, Y., Li, B., Shen, G., Su, Y., Chen, W., Shen, H., Wang, B., and Rong, W.: Occurrence and exposure to polycyclic aromatic hydrocarbons and their derivatives in a rural chinese home through biomass fuelled cooking, Environ. Pollut., 169, 160-166, 2012.

Fan, X., Wei, S., Zhu, M., Song, J., Peng, P. A.: Molecular characterization of primary humic-like substances in fine smoke particles by thermochemolysis–gas chromatography–mass spectrometry, Atmos. Environ., 180, 1-10, 2018.

Fraser, M. P., Lakshmanan, K.: Using levoglucosan as a molecular marker for the long-range transport of biomass combustion aerosols, Environ. Sci. Technol., 34, 4560-4564, 2000.

Gao, Y., Guo, X., Ji, H., Li, C., Ding, H., Briki, M., Tang, L., Zhang, Y.: Potential threat of heavy metals and PAHs in PM2. 5 in different urban functional areas of Beijing, Atmos. Res., 178, 6-16, 2016.

Guo, S., Hu, M., Guo, Q., Zhang, X., Schauer, J., Zhang, R.: Quantitative evaluation of emission controls on primary and secondary organic aerosol sources during Beijing 2008 Olympics, Atmos. Chem. Phys., 13, 8303-8314, 2013.

Hamilton, J., Webb, P., Lewis, A., Hopkins, J., Smith, S., Davy, P.: Partially oxidised organic components in urban aerosol using GCXGC-TOF/MS. Atmos. Chem. Phys., 4, 1279-1290, 2004.

Haque, M., Kawamura, K., Deshmukh, D. K., Fang, C., Song, W., Mengying, B., and Zhang, Y.-L.: Characterization of organic aerosols from a Chinese megacity during winter: predominance of fossil fuel combustion, Atmos. Chem. Phys., 19, 5147-5164, 2019.

Harrison, R. M., Alam, M.S., Dang, J., Ismail, I., Basahi, J., Alghamdi, M. A., Hassan, I., Khoder, M.: Relationship of polycyclic aromatic hydrocarbons with oxy (quinone) and nitro derivatives during air mass transport, Sci. Tot. Environ., 572, 1175-1183, 2016.

He, L.-Y., Hu, M., Huang, X.-F., Zhang, Y.-H., Tang, X.-Y.: Seasonal pollution characteristics of organic compounds in atmospheric fine particles in Beijing, Sci. Tot. Environ., 359, 167-176, 2006a.

He, L.-Y., Hu, M., Huang, X.-F., Zhang, Y.-H., Tang, X.-Y.: Seasonal pollution characteristics of organic compounds in atmospheric fine particles in Beijing, Sci. Tot. Environ., 359, 167-176, 2006b.

Hendricker, A. D., Voorhees, K. J.: Amino acid and oligopeptide analysis using Curie-point pyrolysis mass spectrometry with in-situ thermal hydrolysis and methylation: mechanistic considerations, J. Anal. Appl. Pyrol., 48, 17-33, 1998.

Huang, R.-J., Zhang Y., Bozzetti, C., Ho, F.-H., Cao, J.-J., Han, Y., Daellenbach, K. R., Slowik, J. G., Platt, S. M., Canonaco, F., Zotter, P., Wolf, R., Pieber, S. M., Bruns, E. A., Crippa, M., Ciarelli, G., Piazzalunga, A., Schwikowski, M., Abbaszade, G., Schnelle-Kreis, J., Zimmermann, R., An, Z., Szidat,

S., Baltensperger, U., El Haddad, I., Prevot, A. S. H.: High secondary aerosol contribution to particulate pollution during haze events in China, Nature 514, 218-222, 2014.
Huang, X.-F., He, L.-Y., Hu, M., Zhang, Y.-H.: Annual variation of particulate organic compounds in PM2.5 in the urban atmosphere of Beijing, Atmos. Environ., 40, 2449-2458, 2006.

Keyte, I. J., Harrison, R. M., Lammel, G.: Chemical reactivity and long-range transport potential of polycyclic aromatic hydrocarbons–a review, Chem. Soc.Rev., 42, 9333-9391, 2013.

Ji, D., Yan, Y., Wang, Z., He, J., Liu, B., Sun, Y., Gao, M., Li, Y., Cao, W., Cui, Y., Hu, B., Xin, J., Wang, L., Liu, Z., Tang, G., and Wang, Y.: Two-year continuous measurements of carbonaceous aerosols in urban Beijing, China: Temporal variations, characteristics and source analyses, Chemosphere 200, 191-200, 2018.

Kögel-Knabner, I.: 13C and 15N NMR spectroscopy as a tool in soil organic matter studies, Geoderma 80, 243-270, 1997.

Kong, S., Ji, Y., Liu, L., Chen, L., Zhao, X., Wang, J., Bai, Z., Sun, Z.: Spatial and temporal variation of phthalic acid esters (PAEs) in atmospheric PM_{10} and $PM_{2.5}$ and the influence of ambient temperature in Tianjin, China, Atmos. Environ., 74, 199-208, 2013.

Lang, J., Zhang, Y., Zhou, Y., Cheng, S., Chen, D., Guo, X., Chen, S., Li, X., Xing, X., Wang, H.: Trends of $PM_{2.5}$ and chemical composition in Beijing, 2000-2015, Aerosol Air Qual. Res., 17, 412-425, 2017.

Li, L. J., Ho, S. S. H., Feng, B., Xu, H., Wang, T., Wu, R., Huang, W., Qu, L., Wang, Q., and Cao, J.: Characterization of particulate-bound polycyclic aromatic compounds (PACs) and their oxidations in heavy polluted atmosphere: A case study in urban Beijing, China during haze events, Sci. Tot. Environ., 660, 1392-1402, 2019.

Li, J., Du, H., Wang, Z., Sun, Y., Yang, W., Li, J., Tang, X., Fu, P.: Rapid formation of a severe regional winter haze episode over a mega-city cluster on the North China Plain, Environ. Pollut., 223, 605-615, 2017

Lin, Y., Ma, Y., Qiu, X., Li, R., Fang, Y., Wang, J., Zhu, Y., Hu, D.: Sources, transformation, and health implications of PAHs and their nitrated, hydroxylated, and oxygenated derivatives in $PM_{2.5}$ in Beijing, J. Geophys. Res. Atmos., 120, 7219-7228, doi:10.1002/ 2015JD023628, 2015.

Lv, D., Chen, Y., Zhu, T., Li, T., Shen, F., and Li X.: The pollution characteristics of PM_{10} and $PM_{2.5}$ during summer and winter in Beijing, Suning and Islamabad, Atmos. Pollut. Res., in press, https://doi.org/10.1016/j.apr.2019.01.021, 2019.

Lyu, R., Shi, Z., Alam, M. S., Wu, X., Liu, D., Vu, T. V., Stark, C., Fu, P., Feng, Y., and Harrison, R. M.: Alkanes and aliphatic carbonyl compounds in wintertime $PM_{2.5}$ in Beijing, China, Atmos. Environ., 202, 244-255, 2019.

Lyu, R., Alam, M. S., Stark, C., Xu, R., Shi, Z., Feng, Y., Harrison, R. M.: Aliphatic Carbonyl Compounds (C_8-C_{26}) in Wintertime Atmospheric Aerosol in London, UK, Atmos. Chem. Phys., submitted, 2018a.

762 Lyu, R., Shi, Z., Alam, M. S., Wu, X., Liu, D., Vu, T. V., Stark, C., Fu, P., Feng, Y., Harrison R. M.:
763 Alkanes and aliphatic carbonyl compounds in wintertime $PM_{2.5}$ in Beijing, China, Atmos. Environ.,
764 submitted, 2018b.
765
766 Ma, Y., Cheng, Y., Qiu, X., Cao, G., Fang, Y., Wang, J., Zhu, T., Yu, J., Hu, D.: Sources and oxidative
767 potential of water-soluble humic-like substances (HULIS WS) in fine particulate matter ($PM_{2.5}$) in
768 Beijing, Atmos. Chem. Phys., 18, 5607-5617, 2018.
769
770 Ma, Q., Wu, Y., Zhang, D., Wang, X., Xia, Y., Liu, X., Tian, P., Han, Z., Xia, X., Wang, Y., Zhang,
771 R.: Roles of regional transport and heterogeneous reactions in the $PM_{2.5}$ increase during winter haze
772 episodes in Beijing, Sci. Tot. Environ., 599-600, 246-253, 2017.
773
774 Ogawa, H., Ibuki, T., Minematsu, T., Miyamoto, N.: Diesel combustion and emissions of decalin as a
775 high productivity gas-to-liquid fuel, Energy & Fuels, 21, 1517-1521, 2007.
776
777 Oliveira, T. S., Pio, C., Alves, C. A., Silvestre, A. J., Evtyugina, M., Afonso, J., Fialho, P., Legrand, M.,
778 Puxbaum, H., Gelencsér, A.: Seasonal variation of particulate lipophilic organic compounds at nonurban
779 sites in Europe. J. Geophys. Res.: Atmospheres, 112., D23S09, doi:10.1029/2007JD008504, 2007.
780
781 Oros, D., Simoneit, B.: Identification and emission rates of molecular tracers in coal smoke particulate
782 matter, Fuel 79, 515-536, 2000.
783
784 Pan, S., Wang, L.: Atmospheric oxidation mechanism of m-xylene initiated by OH radical, J. Phys.
785 Chem. A, 118, 10778-10787, 2014.
786
787 Pitts, J. N., Lokensgard, D. M., Ripley, P. S., Van Cauwenberghe, K. A., Van Vaeck, L., Shaffer, S. D.,
788 Thill, A. J., Belser, W. L.: Atmospheric epoxidation of benzo[a]pyrene by ozone: Formation of the
789 metabolite benzo[a]pyrene-4, 5-oxide, Science, 210, 1347-1349, 1980.
790
791 Ren, L., Fu, P., He, Y., Hou, J., Chen, J., Pavuluri, C.M., Sun, Y., Wang, Z.: Molecular distributions
792 and compound-specific stable carbon isotopic compositions of lipids in wintertime aerosols from
793 Beijing, Scientific Rep., 6, 27481, 2016.
794
795 Ringuet, J., Albinet, A., Leoz-Garziandia, E., Budzinski, H., Villenave, E.: Reactivity of polycyclic
796 aromatic compounds (PAHs, NPAHs and OPAHs) adsorbed on natural aerosol particles exposed to
797 atmospheric oxidants, Atmos. Environ., 61, 15-22, 2012.
798
799 Rogge, W. F., Hildemann, L. M., Mazurek, M. A., Cass, G. R., Simoneit, B. R.T .,. Sources of Fine
800 Organic Aerosol. 6. Cigaret Smoke in the Urban Atmosphere, Environ.Sci.Technol., 28, 1375-1388,
801 1994.
802
803 Rogge, W. F., Hildemann, L. M., Mazurek, M. A., Cass, G. R., Simoneit, B. R. T.: Sources of fine
804 organic aerosol. 2. Noncatalyst and catalyst-equipped automobiles and heavy-duty diesel trucks,
805 Environ. Sci.Technol., 27, 636-651, 1993a.
806
807 Rogge, W. F., Mazurek, M. A., Hildemann, L. M., Cass, G. R., Simoneit, B. R. T.: Quantification of
808 urban organic aerosols at a molecular level: Identification, abundance and seasonal variation, Atmos.
809 Environ., Part A., 27, 1309-1330, 1993b.

Ruehl, C. R., Nah, T., Isaacman, G., Worton, D. R., Chan, A. W. H., Kolesar, K. R., Cappa, C. D., Goldstein, A. H., and Wilson, K. R.: The Influence of molecular structure and aerosol phase on the heterogeneous oxidation of normal and branched alkanes by OH, J. Phys. Chem. A., 117, 3990-4000, 2013.

Schauer, J. J., Cass, G. R.: Source apportionment of wintertime gas-phase and particle-phase air pollutants using organic compounds as tracers, Environ. Sci. Technol., 34, 1821-1832, 2000.

Schauer, J. J., Rogge, W. F., Hildemann, L. M., Mazurek, M. A., Cass, G. R., Simoneit, B. R. T.: Source apportionment of airborne particulate matter using organic compounds as tracers, Atmos. Environ., 30, 3837-3855, 1996.

Schmitter, J., Ignatiadis, I., Arpino, P.: Distribution of diaromatic nitrogen bases in crude oils, Geochimica et Cosmochimica Acta, 47, 1975-1984, 1983.

Schwantes, R. H., Schilling, K. A., McVay, R. C., Lignell, H., Coggon, M. M., Zhang, X., Wennberg, P. O., and Seinfeld, J. H.: Formation of highly oxygenated low-volatility products from cresol oxidation, Atmos. Chem. Phys., 17, 3453–3474, 2017.

Shakya, K. M., Griffin, R. J.: Secondary organic aerosol from photooxidation of polycyclic aromatic hydrocarbons, Environ. Sci. Technol., 44, 8134-8139, 2010.

Shen, R., Schäfer, K., Schnelle-Kreis, J., Shao, L., Norra, S., Kramar, U., Michalke, B., Abbaszade, G., Streibel, T., Zimmermann, R., Emeis, S.: Seasonal variability and source distribution of haze particles from a continuous one-year study in Beijing, Atmos. Pollut. Res., 9, 627-633, 2018.

Shen, G., Tao, S., Wei, S., Zhang, Y., Wang, R., Wang, B., Wei, L.I., Shen, H., Huang, Y., and Chen, Y.: Emissions of parent, nitro, and oxygenated polycyclic aromatic hydrocarbons from residential wood combustion in rural China, Environ. Sci. Technol., 46, 8123-8130, 2012a.

Shen, G., Wei, S., Zhang, Y., Wang, R., Wang, B., Li, W., Shen, H., Huang, Y., Chen, Y., and Chen, H.: Emission of oxygenated polycyclic aromatic hydrocarbons from biomass pellet burning in a modern burner for cooking in China, Atmos. Environ., 60, 234-237, 2012b.

Shen, G., Tao, S., Wang, W., Yang, Y., Ding, J., Xue, M., Min, Y., Zhu, C., Shen, H., and Li, W.: Emission of oxygenated polycyclic aromatic hydrocarbons from indoor solid fuel combustion, Environ. Sci. Technol., 45, 3459-3465, 2011.

Simoneit, B. R. T., Kobayashi, M., Mochida, M., Kawamura, K., Lee, M., Lim, H.-J., Turpin, B. J., Komazaki, Y.: Composition and major sources of organic compounds of aerosol particulate matter sampled during the ACE-Asia campaign, J. Geophys. Res.: Atmospheres, 109, D19S10, doi:10.1029/2004JD004598, 2004.

Simoneit, B. R.: Biomass burning - a review of organic tracers for smoke from incomplete combustion, Appl. Geochem., 17, 129-162, 2002a.

Simoneit, B. R. T.: Biomass burning - a review of organic tracers for smoke from incomplete combustion, Appl. Geochem., 17, 129-162, 2002b.

Simoneit, B., Rogge, W., Lang, Q., Jaffé, R.: Molecular characterization of smoke from campfire burning of pine wood (Pinus elliottii), Chemosphere-Global Change Sci., 2, 107-122, 2000.

Simoneit, B. R. T., Sheng, G., Chen, X., Fu, J., Zhang, J., Xu, Y.: Molecular marker study of extractable organic matter in aerosols from urban areas of China, Atmos. Environ., 25, 2111-2129, 1991.

Simoneit, B. R.: Application of molecular marker analysis to vehicular exhaust for source reconciliations, Intl. J.Environ. Anal. Chem., 22, 203-232, 1985.

Simoneit, B. R. T.: Organic matter of the troposphere—III. Characterization and sources of petroleum and pyrogenic residues in aerosols over the western united states, Atmos. Environ., (1967) 18, 51-67, 1984.

Simoneit, B. R., Mazurek, M. A.: Organic matter of the troposphere-II. Natural background of biogenic lipid matter in aerosols over the rural western united states, Atmos. Environ., (1967) 16, 2139-2159, 1982.

Simoneit, B., Schnoes, H., Haug, P., Burlingame, A.: High-resolution mass spectrometry of nitrogenous compounds of the Colorado Green River Formation oil shale, Chem. Geol., 7, 123-141, 1971.

Simpson, C. D., Paulsen, M., Dills, R. L., Liu, L. J. S., Kalman, D. A.: Determination of methoxyphenols in ambient atmospheric particulate matter: Tracers for wood combustion, Environ., Sci. Techno., 39, 631-637, 2005.

Staples, C. A., Peterson, D. R., Parkerton, T. F., Adams, W. J.: The environmental fate of phthalate esters: a literature review, Chemosphere, 35, 667-749, 1997.

Sun, Y., Wang, Z., Fu, P., Yang, T., Jiang, Q., Dong, H., Li, J., Jia, J.: Aerosol composition, sources and processes during wintertime in Beijing, China, Atmos. Chem. Phys., 13, 4577-4592, 2013.

Turpin, B. J., Lim, H.-J.: Species contributions to $PM_{2.5}$ mass concentrations: Revisiting common assumptions for estimating organic mass, Aerosol Sci. Technol., 35, 602-610, 2001.

Wang, J., Ho, S. S. H., Huang, R., Gao, M., Liu, S., Zhao, S., Cao, J., Wang, G., Shen, Z., and Han, Y.: Characterization of parent and oxygenated-polycyclic aromatic hydrocarbons (PAHs) in Xi'an, China during heating period: An investigation of spatial distribution and transformation, Chemosphere, 159, 367, 2016.

Wang, W.: Regional distribution and air-soil exchange of polycyclic aromatic hydrocarbons (PAHs) and their derivatives in Beijing-Tianjin area, Ph.D. Dissertation, Peking University, Beijing, China, 2010.

Wang, G., Kawamura, K., Lee, S., Ho, K., Cao, J.: Molecular, seasonal, and spatial distributions of organic aerosols from fourteen Chinese cities, Environ. Sci. Technol., 40, 4619-4625, 2006.

Wang, G., Kawamura, K.: Molecular characteristics of urban organic aerosols from Nanjing: A case study of a mega-city in China, Environ. Sci. Technol., 39, 7430-7438, 2005.

Wang, Z., Bi, X., Sheng, G., Fu, J.: Characterization of organic compounds and molecular tracers from biomass burning smoke in South China I: Broad-leaf trees and shrubs, Atmos. Environ., 43, 3096-3102, 2009.

Wei, S., Huang, B., Liu, M., Bi, X., Ren, Z., Sheng, G., and Fu, J.: Characterization of $PM_{2.5}$-bound nitrated and oxygenated PAHs in two industrial sites of South China, Atmos. Res., 109, 76-83, 2012.

Welthagen, W., Schnelle-Kreis, J., Zimmermann, R.: Search criteria and rules for comprehensive two-dimensional gas chromatography–time-of-flight mass spectrometry analysis of airborne particulate matter, J. Chromatogr., A 1019, 233-249, 2003.

Wu, X., Vu, T. V., Shi, Z., Harrison, R. M., Liu, D., Cen, K.: Characterization and Source Apportionment of Carbonaceous $PM_{2.5}$ Particles in China - A Review, Atmos. Environ., 189, 187-212, 2018.

Yao, L., Yang, L., Yuan, Q., Yan, C., Dong, C., Meng, C., Sui, X., Yang, F., Lu, Y., Wang, W.: Sources apportionment of PM2. 5 in a background site in the North China Plain, Sci. Tot. Environ., 541, 590-598, 2016.

Yee, L. D., Kautzman, K. E., Loza, C. L., Schilling, K. A., Coggon, M. M., Chhabra, P. S., Chan, M. N., Chan, A. W. H., Hersey, S. P., Crounse, J. D., Wennberg, P. O., Flagan, R. C., Seinfeld, J. H.: Secondary organic aerosol formation from biomass burning intermediates: phenol and methoxyphenols, Atmos. Chem. Phys., 13, 8019-8043, 2013.

Zhang, H., Worton, D. R., Shen, S., Nah, T., Isaacman-VanWertz, G., Wilson, K. R., and Goldstein, A. H.: Fundamental time scales governing organic aerosol multiphase partitioning and oxidative aging, Environ. Sci. Technol., 49, 9768-9777, 2015.

Zhang, Y.-X., Shao, M., Zhang, Y.-h., Zeng, L.-M., He, L.-Y., Zhu, B., Wei, Y., Zhu, X.: Source profiles of particulate organic matters emitted from cereal straw burnings, J.Environ. Sci., 19, 167-175, 2007.

Zhang, Q., Anastasio, C., Jimenez-Cruz, M.: Water-soluble organic nitrogen in atmospheric fine particles (PM2. 5) from northern California, J. Geophys. Res.: Atmospheres, 107, D11, 4112, 10.1029/2001JD000870, 2002.

Zhao, J., Peng, P. A., Song, J., Ma, S., Sheng, G., Fu, J.: Characterization of organic matter in total suspended particles by thermodesorption and pyrolysis-gas chromatography-mass spectrometry, J.Environ. Sci., 21, 1658-1666, 2009.

Zhou, J., Wang, T., Zhang, Y., Zhong, N., Medeiros, P. M., Simoneit, B. R. T.: Composition and sources of organic matter in atmospheric PM10 over a two year period in Beijing, China, Atmos. Res., 93, 849-861, 2009.

TABLE LEGENDS:

Table 1: Comparison of identified organic compounds with earlier studies in Beijing. Data from the present study are mean ± s.d. for n = 33 samples.

Table 2: Molecular formula, diagnostic ions and average concentrations of hopanes identified in $PM_{2.5}$.

Table 3: Estimated average concentrations of unknown compounds (ng m^{-3}) in each section of the chromatogram for haze and non-haze conditions.

FIGURE LEGENDS:

Figure 1: The percentages of the organic compound groups in the total identified organic compounds.

Figure 2: A comparison of organic compound groups between non-haze and haze days. The average total concentration of the identified group was calculated in the non-haze (13 days) and haze periods (20 days), respectively.

Figure 3: The distribution of concentrations of PAHs (shaded bars, 25%-first quartile, 75%-third quartile).

Figure 4: The molecular distributions of aliphatic hydrocarbons and other homologous series, including n-alkanes, branched alkanes, n-alkenes, carbonyl compounds (n-alkanals, n-alkan-2-ones, n-alkan-3-ones), n-alkanoic acid and alkanols on haze and non-haze days.

Figure 5: The molecular distributions of n-C_n-cyclohexane, alkyl-bicyclic-alkanes, alkyl-benzenes, n-C_n-benzenes, alkyl-furanones and alkyl-pyridines on haze and non-haze days.

Figure 6: The concentration (ng m^{-3}) sum of identified and unknown organic compounds in each chromatogram image section during (a) non-haze and (b) haze days.

985 **Table 1:** Comparison of identified organic compounds with earlier studies in Beijing. Data from the
986 present study are mean ± s.d. for n = 33 samples.

	Concentrations, ng m-3	
Compound name	**Present**	**Previous study**
n-alkanols		
1-Dodecanol	2.27±1.49	0.90 j;
1-Tetradecanol	24.2±88.9	3.00 j;
1-Hexadecanol	6.66±20.7	1.2 d; 6.30 j;
1-Octadecanol	1.69±1.65	3.1 d; 20.1 j;
1-Eicosanol	3.71±2.96	19.5 j;
		~~$\sum$ n-alkanols (C_{14}-C_{30}) = 1200 e;~~
n-alkanoic acids		
Hexanoic acid	1.80±1.54	30.4 i; 0.00 j;
Heptanoic acid	0.73±1.05	0.62 j;
Octanoic acid	2.97±2.56	29.6 i; 0.62 j;
Nonanoic acid	1.23±1.37	2.07 j;
Decanoic acid	22.8±25.2	6.4 d; 5.8 i; 1.24 j;
		~~$\sum$ n-alkanoic acid (C_{12}-C_{34}) = 40-11000 e;~~ ~~$\sum$ n-alkanoic acid (C_5-C_{32}) = 426 g;~~ ~~$\sum$ n-alkanoic acid (C_6-C_{22}) = 363 h;~~
Hopanes		
18α(H)22,29,30-trisnorneohopane	2.91±3.06	0.22 j;
17α(H)-22,29,30-Trisnorhopane	1.56±2.74	2.75 a; 2.3 d; 0.5 i; 0.21 j;
17α(H)21β(H)-30-norhopane	9.92±7.63	7.19 a; 4.1 d;
17β(H)21α(H)-hopane(moretane)	5.77±6.12	1.32 j; 1.9 d;
17α(H)21β(H)-hopane	3.71±5.49	3.51 a; 3.2 d; 0.8 i; 1.54 j;
17α(H)21β(H)-homohopane(22R)	1.32±1.31	0.63 a; 1.2 d; 0.42 j;
17α(H)21β(H)-homohopane(22S)	0.83±0.93	2.94 a; 1.2 d; 0.63 j;
17α(H),21β(H)-bishomohopane(22S)	5.23±6.51	0.7 d;
17α(H)21β(H)-bishomohopane(22R)	1.41±1.73	0.7 d;
Subtotal	**32.7±24.7**	
PAHs		
Naphthalene (NAP,2-rings)	6.03±4.52	0.22 b; 2.4 i;
Acenaphthylene (ACY, 2-rings)	12.7±9.93	0.065 b; 0.3 i;
Acenaphthene (ACE, 2-rings)	6.04±8.94	0.79 b; 0.51g; 0.3 i;
Fluorene (FLU, 3-rings)	16.6±13.0	1.18 b; 1.65g; 0.5 i; 15.6 j;
Phenanthrene (PHE, 3-rings)	8.59±8.49	14.0 b; 0.9 d; 1.1 e; 21.65 f; 30.3g; 0.9 i; 95.7 j;
Anthracene (ANT, 3-rings)	6.14±6.53	1.70 b; 3.3 d; 5.74g; 0.2 i; 52.3 j;
Pyrene (PYR, 4-rings)	18.9±18.2	22.3 b; 12 d; 0.58 e; 31.3 f; 64.4g; 1.0 i; 235 j;
Fluoranthene (FLT, 4-rings)	21.0±20.4	41.5 b; 11 d; 0.23 e; 31.8 f; 76.4g; 1.1 i; 222 j;
Chrysene (CHR, 4-rings)	25.5±19.3	21.8 b; 1.00 d; 1.00 e; 50.6 f; 62.7g; 1.3 i; 140 j;
Benz[a]anthracene (BaA, 4-rings)	17.6±14.6	23.5 b; 19 d; 43.4 f; 45.1g; 0.8 i; 62.9 j;

	Concentrations, ng m-3	
Compound name	**Present**	**Previous study**
Benzo[k]fluoranthene (BkF, 4-rings)	8.81±7.68	17.0 b; 8.3 d; 33.6g; 0.7 i; 30.5 j;
Cyclopenta[cd]pyrene (CcP, 5-rings)	8.60±10.2	68.0 j;
Perylene (PER, 5-rings)	3.20±2.69	2.81 b; 14 d; 5.99g; 0.2 i;
Benzo[b]fluoranthene (BbF, 5-rings)	38.5±31.8	34.0 b; 59 d; 33.1 f; 53.6g; 2.3 i; 134 j;
Benzo[a]pyrene (BaP, 5-rings)	13.1±13.8	14.6 b; 14 d; 0.08 e; 40.2 f; 28.6g; 1.1 i; 41.3 j;
Indeno[1,2,3-cd]pyrene (IcdP, 6-rings)	12.3±8.82	18.1 b; 15.2 d; 0.32 e; 40.9 f; 32.3g; 1.2 i; 18.2 j;
Benzo[ghi]perylene (BghiP, 6-rings)	12.4±11.1	12.2 b; 12 d; 0.33 e; 22.2g; 2.6 i; 59.0 j;
Benzo[e]pyrene (BeP, 5-rings)	15.4±10.3	12.4 b; 12 d; 0.65 e; 24.7g; 1.3 i; 72.6 j;
Dibenzo [a,h]pyrene (DBA, 5-rings)	5.68±7.35	2.01 b; 3.1 d;
Benzo[ghi]fluoranthene (BghiF,5-rings)	15.1±15.8	0.08 e; 15.3 f;
O-PAHs		
Anthracenedione (AQ)	5.12±5.97	108 b;
7,12-Benz[a]anthracenequinone (BaAQ)	4.09±3.61	2.14 b;
Aceanthrenequinone (AceAntQ)	2.41±2.89	0.01b;
Phenanthraquinone (PQ)	1.45±1.08	0.13 b;
9-Fluorenone (9-FluQ)	3.78±4.01	28.3g;
Alkylated-(PAHs & OPAHs)		
Pyrene, 1-methyl- (1-MePYR)	21.5±21.5	3.80 b
Phenanthrene, 1-methyl- (1-MePHE)	5.29±5.38	4.29 b
Retene	5.39±9.72	0.12 e; 0.5 i;
Ester		
Dibutyl phthalate (DBP)	16.9±15.5	21 d; 3.00 j;
Diethyl Phthalate (DEP)	2.67±2.91	3.5 d; 24.0 j;
Di(2-ethylhexyl)-phthalate (DEHP)	16.0±12.6	130 d;
Diisobutyl phthalate	49.7±43.2	22 d;
Dimethyl phthalate	2.58±2.80	1.5 d;
Biomarkers		
Levoglucosan	355±232	310 a; 790.3 c; 171 d; 78 h; 97.1 i; 830 j;
Phytone	14.7±11.7	0.9 j;
Phytane	1.94±1.05	2.3 i; 1.30 j;
Pristane	2.24±1.69	1.8 i; 0.67 j;
Other nitrogen compounds (Nitro，amine，heterocyclic compounds)		
Benzo[f]quinoline	4.40±4.66	3.10 j;
Isoquinoline	0.80±0.83	0.22 j;
Phenolic compounds		
1-Naphthalenol (1-OH-NAP)	1.56±5.61	0.22 b
2-Naphthalenol (2-OH-NAP)	1.15±1.21	2.74 b
2-Dibenzofuranol (2-OHDBF)	1.84±2.09	1.47 b

a. Beijing, PKU, Heating seasons (Ma et al., 2018);
b. Beijing, PKU, Heating seasons (Lin et al., 2015);
c. Beijing, China University of Geosciences (Beijing), winter (Shen et al., 2018);
d. Beijing, winter of 2003 (Wang et al., 2006)
e. Beijing, urban, June (Simoneit et al., 1991);
f. Beijing, urban, haze period (Gao et al., 2016);
~~f.~~g. Beijing, PKU, haze period (Li et al., 2019);
~~g.~~h. ~~Beijing, PKU, winter (Huang et al., 2006);~~
~~h.~~i. Beijing, PKU, winter (He et al., 2006b)
~~i.~~j. During the 2008 Beijing Olympic Games, PKU sites, (Guo et al., 2013);
~~j.~~k. Beijing, urban, winter (Zhou et al., 2009);
~~Beijing, PKU, winter (Huang et al., 2006);~~

Table 2: Molecular formula, diagnostic ions and average concentrations of hopanes identified in $PM_{2.5}$.

Compounds		Molecular formula	Diagnostic ions	IAP, ng m^{-3}
18α(H)22,29,30-trisnorneohopane	Ts	$C_{27}H_{46}$	191/370	2.91 ± 3.06
17α(H)-22,29,30-Trisnorhopane	Tm	$C_{27}H_{46}$	191/370	1.56 ± 2.74
17α(H)21β(H)-30-norhopane	29αβ	$C_{29}H_{50}$	191/398	9.92 ± 7.63
17β(H)21α(H)-hopane(moretane)	30βα	$C_{30}H_{52}$	191/412	5.77 ± 6.12
17α(H)21β(H)-hopane	30αβ	$C_{30}H_{52}$	191/412	3.71 ± 5.49
17α(H)21β(H)-homohopane(22R)	30αβ-22R	$C_{31}H_{54}$	191/426	1.32 ± 1.31
17α(H)21β(H)-homohopane(22S)	30αβ-22S	$C_{31}H_{54}$	191/426	0.83 ± 0.93
17α(H),21β(H)-bishomohopane(22S)	30αβ-22S	$C_{32}H_{56}$	191/440	5.23 ± 6.51
17α(H)21β(H)-bishomohopane(22R)	30αβ-22R	$C_{32}H_{56}$	191/440	1.41 ± 1.73

Table 3: Estimated average concentrations of unknown compounds (ng m^{-3}) in each section of the chromatogram for haze and non-haze conditions.

Section	Characteristics of organic compounds	Non-haze		Haze	
		Total	**Unidentified**	**Total**	**Unidentified**
1	Low molecular weight: ➢ carbon numbers (n-alkanes) ≤ 17; ➢ monoaromatics;	802	546	911	632
2	Medium molecular weight: ➢ 17 < carbon numbers (n-alkanes) ≤ 23); ➢ Oxidized hydrocarbons (alkanals, alkanones);	334	137	483	147
3	Medium molecular weight: ➢ 23 < carbon numbers (n-alkanes) ≤ 27); ➢ Oxidized hydrocarbons (alkanals, alkanones);	573	215	1060	228
4	High molecular weight: ➢ carbon numbers (n-alkanes) ≥ 27;	351	188	730	320
5	Oxidized monoaromatics;	621	289	1309	985
6	2 rings PAHs	485	303	1556	879
7	3-6 rings PAHs and hopanes;	792	440	1337	774
	Total	3958	2119	7385	3964

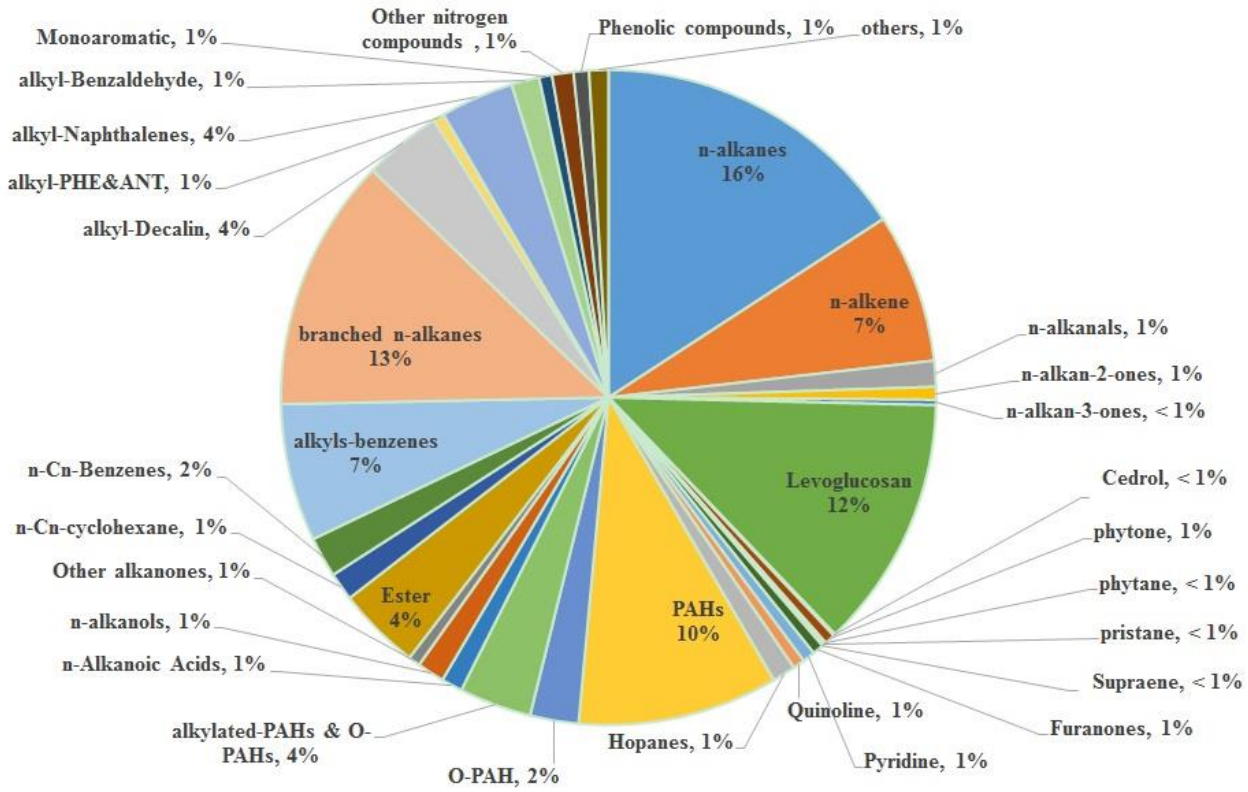

Figure 1: The percentages of the organic compound groups in the total identified organic compounds.

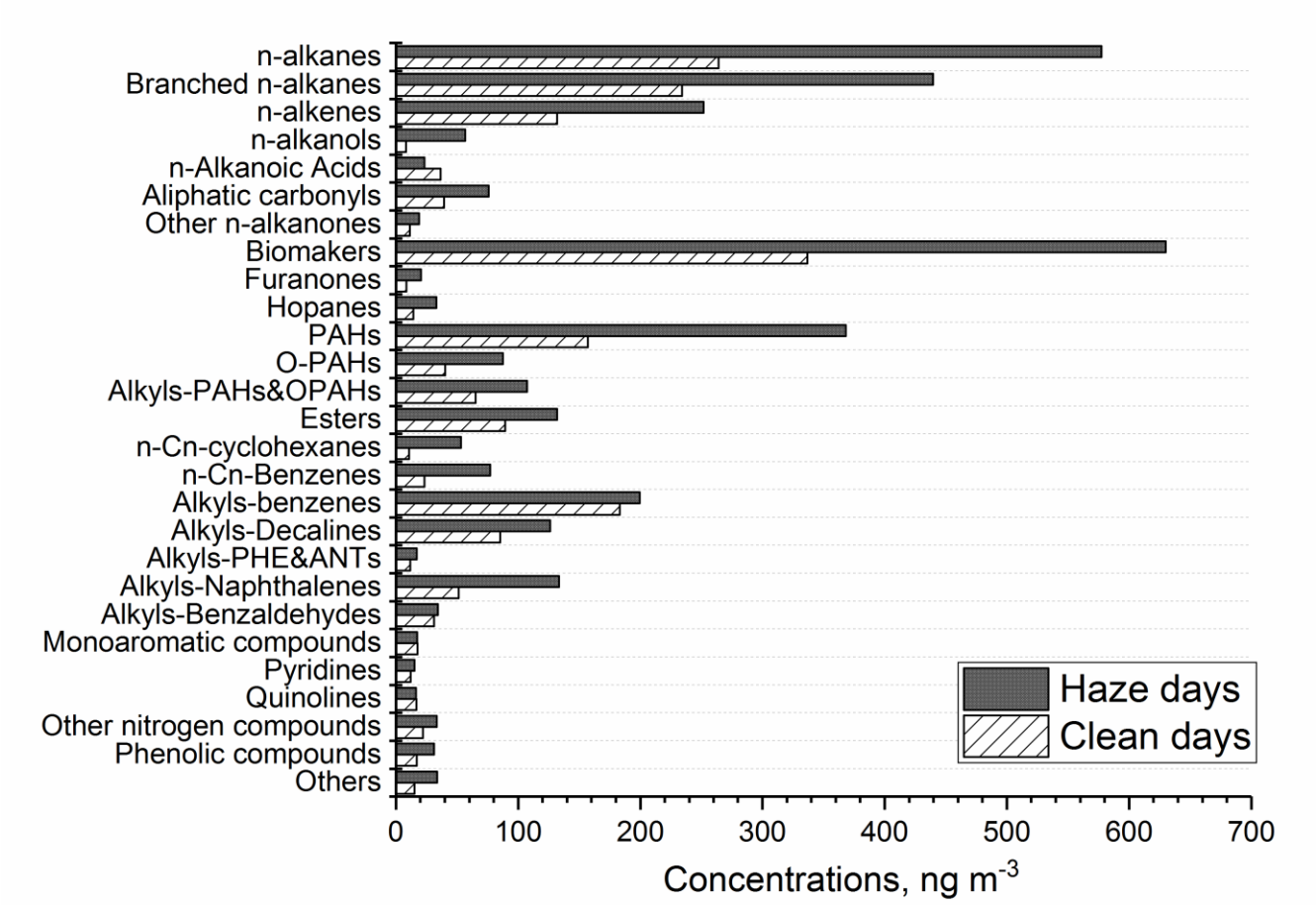

Figure 2: A comparison of organic compound groups between non-haze and haze days. The average total concentration of the identified group was calculated in the non-haze (13 days) and haze periods (20 days), respectively.

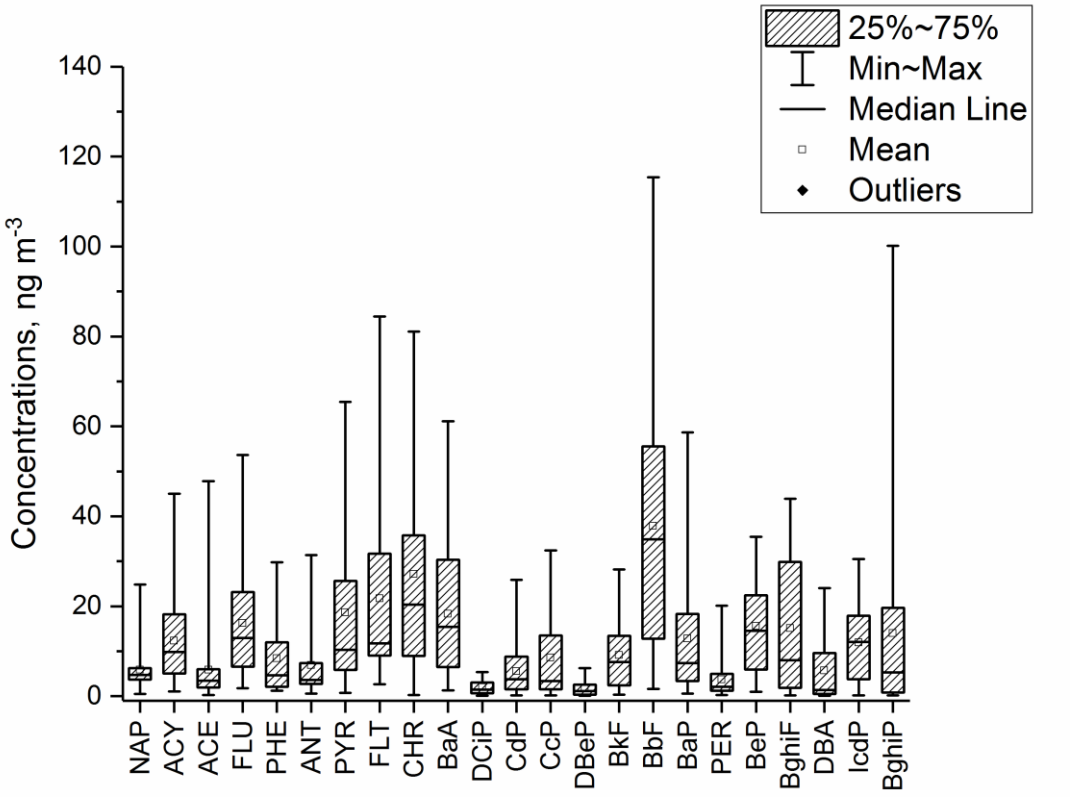

1017

1018 **Figure 3:** The distribution of concentrations of PAHs (shaded bars, 25%-first quartile, 75%-third
1019 quartile).
1020

1021

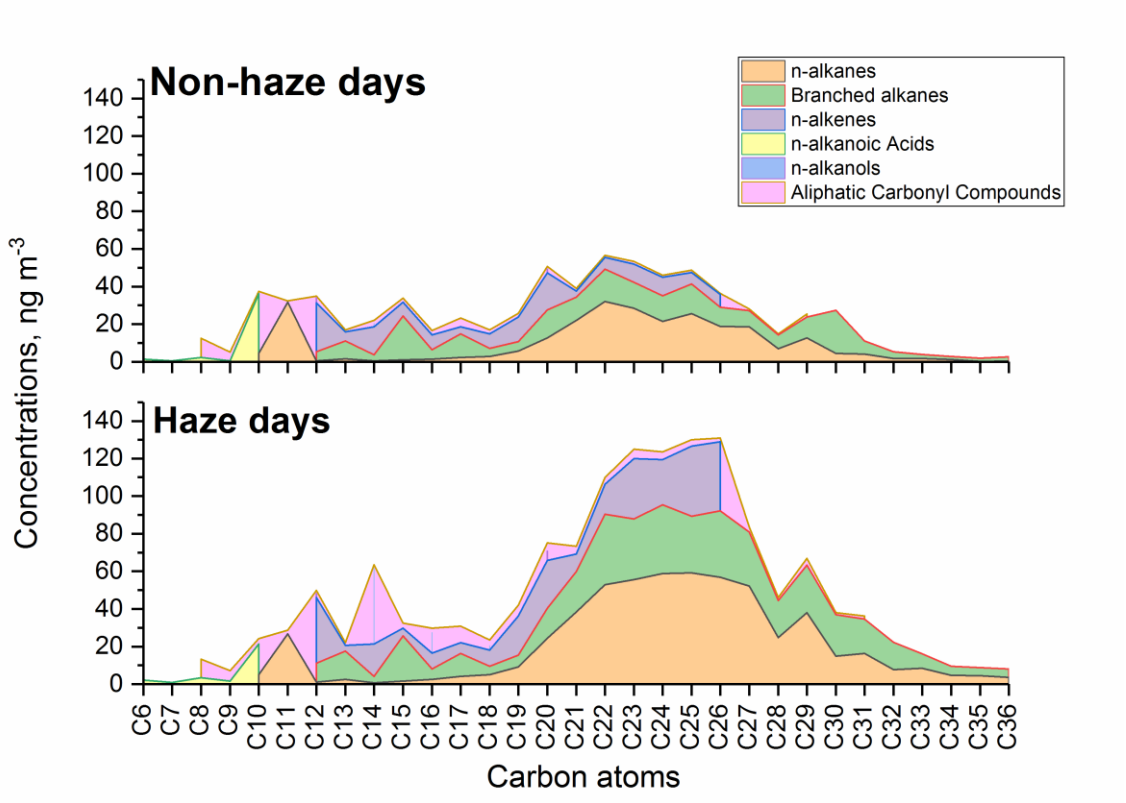

Figure 4: The molecular distributions of aliphatic hydrocarbons and other homologous series, including n-alkanes, branched alkanes, n-alkenes, carbonyl compounds (n-alkanals, n-alkan-2-ones, n-alkan-3-ones), n-alkanoic acid and alkanols on haze and non-haze days.

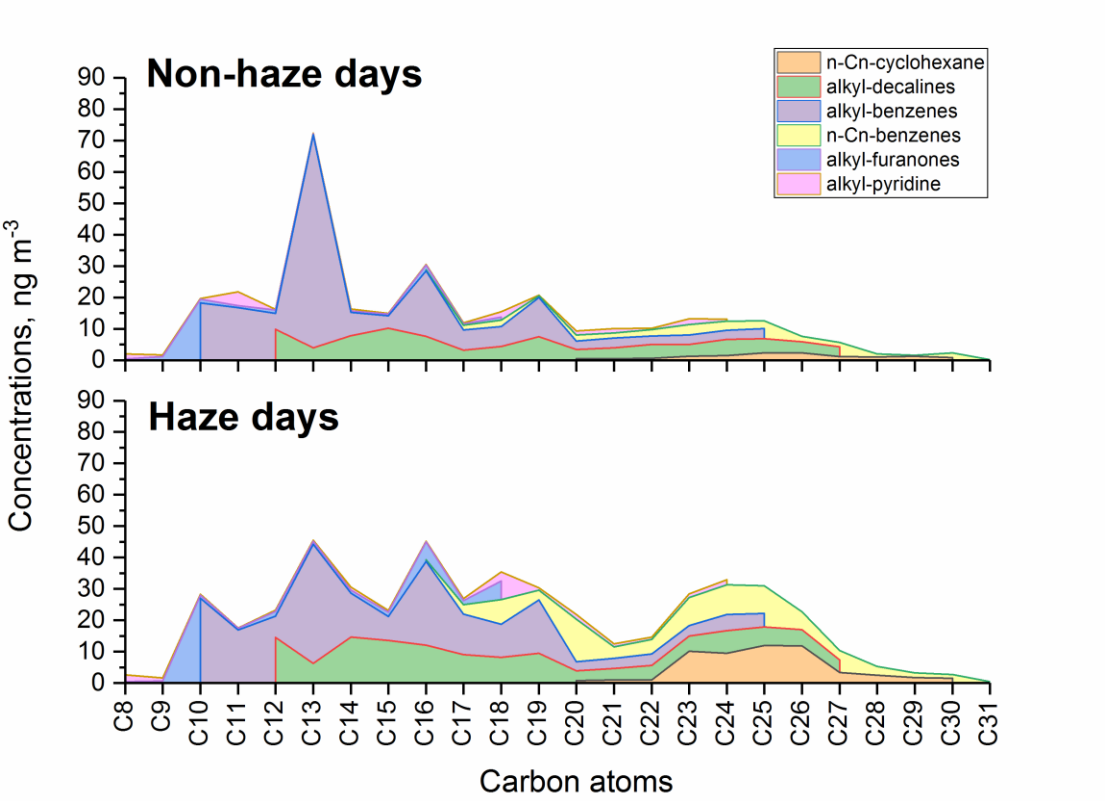

Figure 5: The molecular distributions of n-C_n-cyclohexane, alkyl-bicyclic-alkanes, alkyl-benzenes, n-C_n-benzenes, alkyl-furanones and alkyl-pyridines on haze and non-haze days.

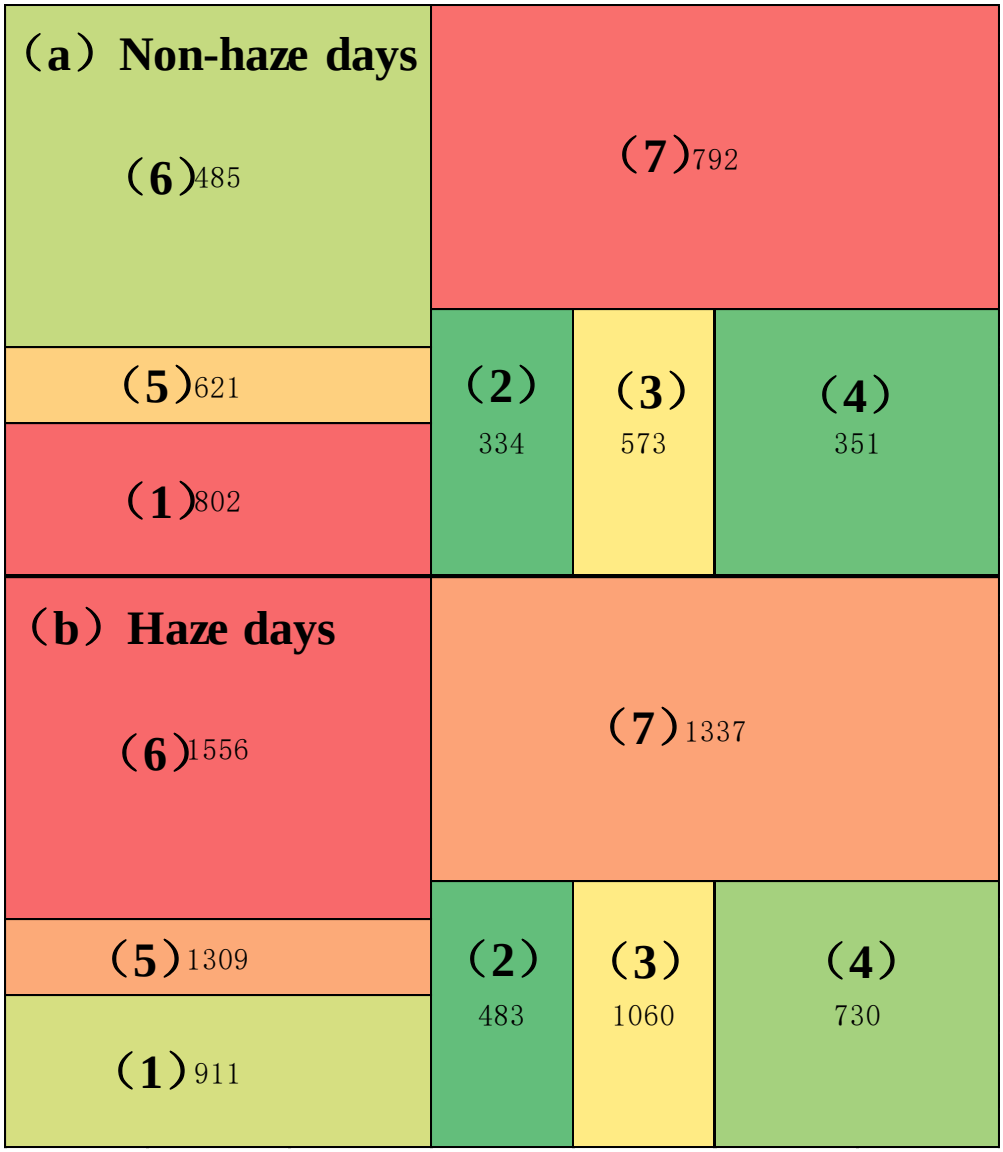

Figure 6: The concentration (ng m^{-3}) sum of identified and unknown organic compounds in each chromatogram image section during (a) non-haze and (b) haze days.